Coordination Chemistry Reviews 255 (2011) 2746–2763

Contents lists available at ScienceDirect

Coordination Chemistry Reviews

journal homepage: www.elsevier.com/locate/ccr

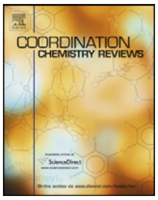

Review

Inorganic metallocenes: The structures and aromaticity of sandwich compounds of the transition elements with inorganic rings

Edward Maslowsky Jr.[*]

Department of Molecular and Life Sciences, Loras College, Dubuque, IA 52001, United States

Contents

---

[*] Corresponding author. Tel.: +1 563 588 7041.
E-mail address: Edward.Maslowsky@loras.edu

doi:10.1016/j.ccr.2011.04.011

ARTICLE INFO

Article history:
Received 29 July 2010
Accepted 21 April 2011
Available online 30 April 2011

Keywords:
Aromatic compounds
Coordination compounds
Covalent bonding
Metallocenes
Resonance
Transition elements

ABSTRACT

The concept of aromaticity has dramatically evolved and expanded to where it is no longer reserved for use in organic chemistry but is also useful in describing the bonding in many inorganic compounds. The aromaticity of inorganic rings arises from participation of s, p, d and f atomic orbitals to form delocalized σ, π, δ and φ molecular orbitals. This report describes the stability, structures and bonding of mainly covalent inorganic "sandwich" compounds or metallocenes in which aromatic, antiaromatic and nonaromatic inorganic rings, as well as those with multiple or conflicting aromaticity, are bonded primarily to the transition elements. Also included are some examples of ionic salt and covalent metallocenes of the main group and f-block elements with rings that exhibit other than only p orbital aromaticity. While many of the referenced compounds have been experimentally generated, computational methods play an important role in predicting the stability and ground state structures of several other hypothetical inorganic rings and the metallocenes produced from them. The theoretical studies also aid in defining the criteria that are used in determining the nature of compound aromaticity.

1. Introduction

The convergence of several developments has fostered an emerging interest in inorganic "sandwich" compounds or metallocenes. The first was the introduction of the concept of aromaticity in organic chemistry [1]. The most well known aromatic compound, benzene, was isolated by Faraday in 1825 [2], with the concept of aromaticity itself introduced by Kekulé in the 1860s [3].

The development of molecular orbital theory by Hückel in the 1930s [4] led to the formulation of the Hückel rule [5] as a general method of defining aromaticity in conjugated organic rings such as benzene as requiring $4n+2$ π-electrons (where n is an integer). These delocalized electrons are located in parallel atomic p orbitals found on the ring atoms of C and some other nonmetallic elements. Conjugated rings with $4n$ π-electrons are characterized as antiaromatic if planar as in cyclobutadiene, or nonaromatic if nonplanar as in cyclooctatetraene [6,7].

Though introduced almost one and a half centuries ago, there is at present no single generally accepted definition of the term aromatic [1a,8–11]. Efforts to develop more quantitative definitions have led to the characterization of several different types of aromaticity that are found in an even greater variety of organic and inorganic compounds. Indeed, one recent report describes ten different types of aromaticity [9]. The identification of aromaticity is based on a variety of criteria that use chemical (with aromatic compounds more likely than other unsaturated organic compounds to undergo substitution rather than addition reactions), structural (equal ring bond lengths), electronic (molecular orbital pattern, electron delocalization, electronic excitation, electronic excitations and orbital eigenfunctions) and magnetic properties (magnetic susceptibility anisotropies and ^{1}H NMR chemical shifts) [10,12–14]. A chronology of the criteria used to define aromaticity and of its historical development has recently appeared [15]. It is sometimes difficult to correlate the various criteria, and the use of different criteria can produce contradictory conclusions about the aromaticity of some molecules [12].

A second development within the last approximately 15 years has been the rapid advancement and increased popularity of computational methods such as density functional theory (DFT) calculations to determine global minimum structures and as an aid in defining aromatic criteria and characterizing the nature and extent of atomic orbital contributions to aromaticity [9]. As recently noted, however, although progress in this area has led to predictions of new molecules that might contradict chemical intuition, the proposed molecular structures may not represent the global minimum, and the experimental preparation of these species may be difficult or impossible [16,17]. The computational analyses are sometimes supported with experimental photoelectron spectral data of compounds generated as gaseous species [11,18].

As a result, to traditional π-aromaticity arising from electron delocalization in parallel p orbitals have been added σ-aromaticity resulting from s, p, d and f orbital participation, π- and δ-aromaticity from d and f orbital participation and φ-aromaticity from f orbital participation. Multiple aromaticity, multiple antiaromaticity and conflicting aromaticity have also been characterized [11,19–23]. The characterization of these bonding modes in metallic systems has produced additional electron counting rules for cyclic transition metal compounds [21–23].

In 1996 Schleyer and co-workers reported the development of what has become one of the most commonly used of the magnetic criteria to evaluate the aromatic or antiaromatic character of both organic and inorganic rings [13,24]. It allows for the determination of nucleus-independent chemical shift (NICS) values that are the negative of the shielding calculated at the geometric ring center (NICS(0) values) or some other part of a molecule; most commonly 1 Å above the ring center (NICS(1) values) [9,12]. While negative NICS values indicate aromatic character, positive NICS values indicate antiaromatic character. Characteristic of nonaromatic compounds is the absence of delocalization and NICS values close to zero.

Several NICS based aromatic indexes have been developed that provide more accurate and complete measures of molecular aromaticity [10]. These NICS based approaches continue to evolve in an attempt to produce quantitative methods that accurately describe the aromatic character of compounds. One study has evaluated five NICS based aromatic indexes against a uniform set of aromatic stabilization energies for 75 mono- and polyheterocyclic five-membered rings with planar global minimum structures [25]. It concluded that the value of the π component of the out-of-plane zz shielding tensor, $\mathrm{NICS}(0)_{\pi zz}$, is superior for planar inorganic and organic rings and cages since it eliminates contributions of non-π contributions to aromaticity. The more readily obtained and easy to use $\mathrm{NICS}(1)_{zz}$ index was offered as a good alternative [10,25]. This has in turn resulted in the use of NICS_{zz}-scan curves produced by plotting NICS_{zz}-scan values along the principle symmetry axis of the ring plane to probe the aromatic and antiaromatic behavior of several cyclic organic, inorganic and all-metal molecules [26–28]. The need for further refinements is illustrated by the use of the recently developed Adaptive Natural Density Partitioning (AdNDP) method [29] to show that the aromaticity proposed for Re_3Cl_6 [30] and Tc_3X_9 (X = Cl, Br) [31] clusters through the use of standard NICS methods was incorrect.

A third development, the report in 1951 of the first sandwich compound, ferrocene ($(\eta^5\text{-}C_5H_5)_2Fe$) [32,33], has led to the

Table 1
NICS(0) and NICS(1) values (ppm) for the most stable isomers of the *cyclo*-Be_3^{2-} dianion in the isolated state and in several metal salts calculated at the B3LYP/6-311+G(d) level [35,36].

	Be_3^{2-} (D_{3h})	$[MBe_3]^-$ (C_{3v})			M_2Be_3 (D_{3h})			$[(\eta^3\text{-}Be_3)_2M_2]^{2-}$ (D_{3h})	
		M = Li	Na	Cu	M = Li	Na	Cu	M = Be	Zn
NICS(0)	−65.06	−38.88	−35.38	−43.48	−42.05	−45.01	−47.25	−38.112	−37.009
NICS(1)	−31.82	−32.76	−35.32	−89.87	−25.28	−28.28	−90.82	−19.750	−19.536

synthesis of countless ionic and covalent organometallic compounds that have from three to nine atom organic rings. These rings have a variety of different substituents and interact with metal centers using several different bonding modes. They also sometimes achieve stability on complex formation that is not possible in the isolated state. Since their discovery, metallocenes and other organometallic compounds have come to play a very important role in extending our understanding of chemical bonding. Practical applications include their use as synthetic reagents, catalysts for polymer production and building blocks for new materials.

Aromatic rings and metallocenes are no longer the exclusive prerogative of organic chemistry. Borazine (Fig. 1), which was synthesized in 1926 [34], is the first example of what was originally presented as an inorganic aromatic compound. However, as the last decades of the 20th century ended and the 21st century has begun, interest in the preparation and characterization of inorganic rings and sandwich compounds in which inorganic rings interact with metal-centers has grown rapidly.

This report describes the structures and aromaticity of mainly covalent transition element metallocenes of inorganic rings. That almost two thirds of the cited references have a publication date of 2000 or later, and approximately a third of these have appeared in the last 5 years illustrates the current interest in these compounds. While several are of experimentally generated compounds, a large number are also of hypothetical compounds that are studied theoretically using computational methods. Could these compounds serve as catalysts or nanomaterials or in other novel capacities? One can only speculate as to whether the development of practical applications arising from the discovery of organic metallocenes at the middle of the last century will be equally as fruitful for inorganic metallocenes as the present century unfolds.

2. *Cyclo*-X_3 ligands

2.1. Group 2 element rings

The *cyclo*-Be_3^{2-} dianion is aromatic according to the Hückel rule with 2 π-electrons and maintains its aromaticity and planar structure in the bimetallic species $[MBe_3]^-$ and M_2Be_3 (M = Li, Na, Cu). Calculated NICS values (Table 1) indicate that the aromaticity of the *cyclo*-Be_3^{2-} dianion decreases on complex formation [35]. A structure with C_{3v} symmetry is most stable for $[MBe_3]^-$ (M = Li, Na, Cu) (Fig. 2a), while a structure with D_{3h} symmetry is most stable for M_2Be_3 (M = Li, Na, Cu) (Fig. 2b). Calculations also show the stability of the highly aromatic sandwich compounds $[(\eta^3\text{-}Be_3)_2M_2]^{2-}$ (M = Be [36], Zn [35]) in which the *cyclo*-Be_3^{2-} units are eclipsed to give D_{3h} symmetry structures.

The first report of aromaticity in a group 2 atom ring was in a theoretical study of the Mg_3^- anion and of the two clusters $NaMg_3^-$ (Fig. 2a) and Na_2Mg_3 (Fig. 2b) that contain the *cyclo*-Mg_3^{2-} dianion [37]. The aromaticity of these clusters arises from π-electrons that produce π-aromaticity without the formation of a σ-framework. A more recent theoretical study, however, concluded that the isolated *cyclo*-Mg_3^{2-} unit possesses only σ-aromaticity [38]. In a theoretical study of the series of complexes $[X_nM_3]^{n-2}$ (M = Be, Mg, Ca; X = Li, Na, K; n = 0–2), it was reported that the aromaticity found in the three-center two-electron ring of the isolated *cyclo*-M_3^{2-} units is not only stabilized on interaction with alkali metals, but also changes from σ-aromaticity to π-aromaticity [39]. The aromaticity could be further tuned by changing the perpendicular distance between X and the center of the M_3 ring. This was especially true for Na_2Mg_3, Li_2Mg_3 and X_2Be_3, while X_2Be_3 and K_2Mg_3 are much less likely to exhibit changes in aromaticity through small changes in this distance. These observations were felt to be important since the ability to change aromaticity might influence the reactivity of all-metal aromatic clusters. A theoretical study has explored changes in aromaticity, as well as in reactivity and bonding patterns, observed in a reaction cycle involving eleven different reactions in which one or both *cyclo*-$C_5H_5^-$ anions in $(\eta^5\text{-}C_5H_5)_2Ti$ were successively replaced by *cyclo*-Be_3^{2-} and *cyclo*-Mg_3^{2-} units [40]. The resulting products were $[\eta^5\text{-}C_5H_5TiX_3]^-$, $[(\eta^3\text{-}X_3)_2\ Ti]^{2-}$ (X = Be, Mg) and $[(\eta^3\text{-}Be_3)Ti(\eta^3\text{-}Mg_3)]^{2-}$.

2.2. Group 13 element rings

It has been suggested that the aromatic 2 π-electron *cyclo*-$B_3H_6^+$ cation, which is an isoelectronic analogue of the *cyclo*-$C_3H_3^+$ cation, is capable of forming π-complexes (Fig. 2c) with different main group and transition elements, and calculations have shown that $(\eta^3\text{-}B_3H_6)Co(CO)_3$ is stable with the three terminal and three bridging H atoms bent out of the *cyclo*-B_3 plane and away from the Co atom [41].

The first "cycloaluminene", $Na_2[Al_3R_3]$ (R = C_6H_3-2,6-(C_6H_2-2,4,6-$Me_3)_2$) has been synthesized [42]. Although NICS data were not determined, the presence of a delocalized molecular orbital with 2 π-electrons suggests that the *cyclo*-Al_3^{2-} unit is aromatic.

Reported canonical molecular orbital NICS values (Table 2) show that the $[Al_3H_3]^{2-}$ dianion exhibits both π- and σ-aromaticity [43]. However, this study also noted a previous observation [44] that the tendency of small Al ring clusters to collapse to form larger clusters is a problem to be considered in determining the ability of cyclotrialane rings to form sandwich compounds. Although bulky R groups

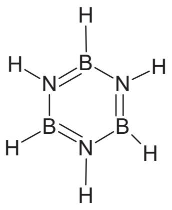

Fig. 1. Molecular structure of borazine.

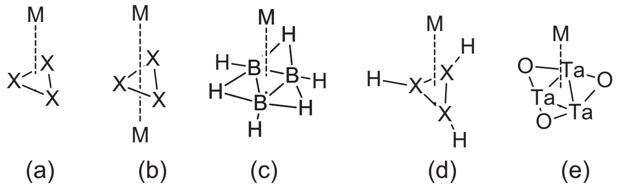

Fig. 2. Common ring structures of complexes with *cyclo*-X_3 ligands or cores.

Table 2
NICS(0) and NICS(1) values (ppm) for $[Al_3R_3]^{2-}$ (R = H, F) dianions in the isolated state and the most stable isomers of several metal salts computed at the B3LYP/6-311+G(2df) level [43].

	$[Al_3R_3]^{2-}$		$[(\eta^3\text{-}Al_3R_3)_2Al]^-$		$Na_2[(\eta^3\text{-}Al_3F_3)_2Ti]$	$Na_2[(\eta^3\text{-}Al_3F_3)_2M_2]$	
	R = H	F	R = H	F		M = Mg	Zn
Symmetry	D_{3h}	D_{3h}	D_{3h}	D_{3h}	D_{3d}	D_{3h}	D_{3d}
NICS(0)	−13.04	−45.14	−1.34	−24.87	−35.51	−36.84	−36.49
NICS(1)	−11.02	−27.61	−7.68	−14.40	−22.54	−18.29	−21.66

stabilize cyclotrialane rings in $[Al(\eta^3\text{-}Al_3R_3)_2]^-$ ($R = N(SiMe_3)_2$) [45] and the radical $[Al(\eta^3\text{-}Al_3R_3)_2]^{\bullet}$ ($R = N(SiMe_2Ph)_2$) [46], the *cyclo*-$Al_3R_3{}^{2-}$ dianions do not maintain their aromaticity in these complexes. Other ring substituents, however, can dramatically increase the aromaticity of *cyclo*-$Al_3R_3{}^{2-}$ molecules relative to that of *cyclo*-$Al_3H_3{}^{2-}$ [43]. They can also make the D_{3h} symmetry structure the most stable isomer [43], although it is not the most stable isomer for $[Al_3H_3]^{2-}$ [47,48].

As a result, calculations show the expected stability of the sandwich complexes $[Al(\eta^3\text{-}Al_3F_3)_2]^-$, $Na_2[Ti(\eta^3\text{-}Al_3F_3)_2]$ and $Na_2[M_2(\eta^3\text{-}Al_3F_3)_2]$ (M = Mg, Zn), and that the *cyclo*-$Al_3F_3{}^{2-}$ units (Table 2) retain their aromaticity in these complexes [43]. While the rings are staggered in the charge-compensated Ti (Fig. 3a) and Al complexes, they are eclipsed in the charge-compensated Zn (Fig. 3b) and Mg complexes [43]. It was suggested that gas-phase investigations may be used to prepare these and other species in which different substituents are added to the rings or various ligands are attached to the coordination sphere of the complexed metal.

The first reported examples of compounds exhibiting metalloaromaticity are the ionic complexes $M_2[(Mes_2C_6H_3)Ga]_3$ ($Mes = 2,4,6\text{-}Me_3C_6H_2$; M = Na [49], K [50]) prepared by Robinson and coworkers. Like the analogous Al compounds, they contain trisubstituted, non-bridged *cyclo*-$Ga_3{}^{2-}$ cores that exhibit aromatic character. Their ability to form sandwich compounds has yet to be explored.

2.3. Group 14 element rings

Calculations show the stability of non-hydrogen-bridged ring structures in $(\eta^3\text{-}X_3H_3)M$ (X = C, Si, Ge; M = $Co(CO)_3$, $Rh(CO)_3$, $Ir(CO)_3$, $Ni(CO)_3$, $Co(PH_3)_3$, $Ni(PH_3)_3$) (Fig. 2d), and of non-methyl-bridged ring structures in $[\eta^3\text{-}X_3(CH_3)_3]Co(CO)_3$ (X = Si, Ge) [51]. While ligand-to-metal charge transfer produces cationic ligands in complexes where X = Si and Ge, a small metal-to-ligand charge transfer produces an anionic ligand for X = C.

2.4. Group 15 element rings

A theoretical analysis of $[(\eta^3\text{-}N_3)_2Ni]^{2-}$, $[(\eta^3\text{-}N_3)_2M(CO)_2]^q$ (M, q) = (Fe, 0), (Mn, 1-), $[(\eta^3\text{-}N_3)M(CO)_3]^q$ ((M, q) = (Co, 0), (Fe, 1-)) and $[(\eta^3\text{-}N_3)M(\eta^5\text{-}C_5H_5)]^q$ ((M, q) = (Ni, 0), (Co, 1-)) has determined that the polynitrogen cluster is present not as the aromatic and singlet *cyclo*-$N_3{}^+$ cation with 2 π-electrons but as the triplet diradical *cyclo*-$N_3{}^-$ anion with 4 π-electrons [52]. The NICS(1) values show that the triplet *cyclo*-$N_3{}^-$ anion is aromatic and maintains its aromaticity in the transition metal complexes. Indeed, it has previously been noted [11,53] that the electron count for aromaticity in triplet state species is not $4n+2$ but $4n$. On complex formation, the two unpaired electrons on the free triplet *cyclo*-$N_3{}^-$ anion are evenly distributed over the entire ring to become part of the bonding interaction with the transition metal atoms of the seven complexes. As a result, all complexes have the singlet ground state. After speculating about possible experimental routes for preparing these complexes, it was concluded that successful synthesis would be especially likely for the complexes $[(\eta^3\text{-}N_3)M(\eta^5\text{-}C_5H_5)]^q$ ((M, q) = (Ni, 0), (Co, 1-)). Indeed, it is not unusual to find that the $\eta^5\text{-}C_5H_5{}^-$ ligand stabilizes complexes containing inorganic rings. Calculations show the stability of $(\eta^3\text{-}N_3)Sc$ with C_{3v} symmetry in the singlet ground state [54].

Several covalent transition element complexes have been synthesized with planar $\eta^3\text{-}X_3$ (X = P [55–59], As [57,59–61], Sb [62]) rings (Fig. 2a). These complexes have been described as containing either neutral nonaromatic 3 π-electron $\eta^3\text{-}X_3$ rings [61], or, at the ionic limit, aromatic 6 π-electron $\eta^3\text{-}X_3{}^{3-}$ rings [63]. A complex of Nb has recently been reported that is able to shuttle the P_3 ligand to change $AsCl_3$ into AsP_3 [64].

Transition metal complexes with heteroatom $\eta^3\text{-}P_2X$ (X = As [57,58], Sb) [56] and $\eta^3\text{-}As_2P$ [57] rings have also been characterized.

Inverse homo- and hetero-metal sandwich complexes containing $\mu\text{-}(\eta^3\text{:}\eta^3\text{-}X_3)$ ligands (X = P [55,59,61,65], As [60]) (Fig. 2b) have been prepared. Molecular orbital data show that stable complexes require from 30 to 34 valence electrons [66,67] and that those with 31 to 33 valence electrons are expected to exhibit a Jahn–Teller distortion due to a doubly degenerate ground electronic state [65]. Complexes are also found with *cyclo*-X_3 ligands that bridge transition metal atoms using η^2- (X = P [68–70], As [71]) or η^1-bonding (X = P [61,69], As [71]).

2.5. Group 16 element rings

An energy mismatch between *cyclo*-X_3 (X = O, S) ligand donor and transition metal carbonyl fragment acceptor orbitals produces unstable complexes. Calculations show a reduction in this mismatch on replacing one or more weak π-acceptor CO ligands with the very strong π-acceptor NO^+ ligand to produce stable $[(\eta^3\text{-}O_3)M(NO)_3]^{3+}$ (M = Cr, Mo, W, Fe, Ru, Os), $[(\eta^3\text{-}S_3)W(NO)_3]^{3+}$ and $[(\eta^3\text{-}S_3)W(NO)_2(CO)]^{2+}$ [63].

Slightly unequal Te–Te bond lengths are present in the antiaromatic 4 π-electron *cyclo*-$Te_3{}^{2+}$ unit in $[(\eta^3\text{-}Te_3)M(CO)_4](SbF_6)_2$ (M = W [72], Mo [73]) (Fig. 4).

2.6. d- and f-block element rings

Calculations show the expected stability of the 1:1 and 2:1 sandwich-type complexes formed through the interaction of the

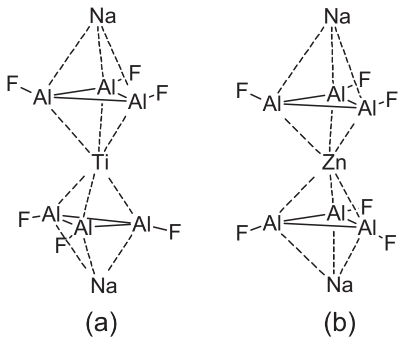

Fig. 3. Optimized structures of (a) $Na_2[Ti(\eta^3\text{-}Al_3F_3)_2]$ and (b) $Na_2[Zn(\eta^3\text{-}Al_3F_3)_2]$ [43].

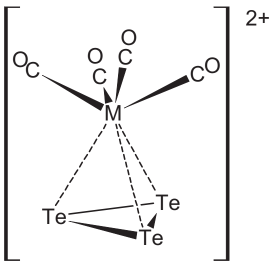

Fig. 4. X-ray crystal structure of $[(\eta^3\text{-Te}_3)\text{M(CO)}_4](\text{SbF}_6)_2$ (M = W [72], Mo [73]).

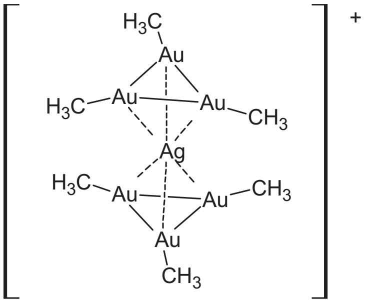

Fig. 5. Equilibrium geometry of S_6 symmetry calculated for $[\{\eta^3\text{-Au}_3(\text{CH}_3)_3\}_2\text{Ag}]^+$ [74].

aromatic *cyclo*-Au_3 cluster in *cyclo*-$Au_3L_nH_{3\text{-}\boldsymbol{n}}$ (L = CH_3, NH_2, OH, Cl; *n* = 1–3) with electrophiles [74]. While a staggered orientation of the *cyclo*-Au_3 clusters is found to be most stable in the 2:1 complexes $[\{\eta^3\text{-Au}_3(\text{CH}_3)_3\}_2\text{M}]^+$ (M = Li, Tl, Ag (Fig. 5)) and $[\{\eta^3\text{-Au}_3(\mu_2\text{-NH}_2)_3\}_2\text{Li}]^+$, the eclipsed conformation is most stable in $[\{\eta^3\text{-Au}_3(\mu_2\text{-NH}_2)_3\}_2\text{Tl}]^+$. The ring-interactions are predominantly electrostatic with Li^+ and Tl^+ ions and covalent with Ag^+. Contributions from the Au atom 6s orbitals produce σ-aromaticity, while contributions from the 5d orbitals produce σ-, π- and δ-aromaticity in the η^3-Au_3 rings.

A molecular orbital study based on photoelectron spectroscopy and DFT data shows both π- and δ-aromaticity but no σ-aromaticity from Ta atom 5d orbital participation in the *cyclo*-Ta_3 core of $[\text{Ta}_3(\mu_2\text{-O})_3]^-$ [75]. The possibility of δ-aromaticity in other cyclic complexes of low oxidation state transition metals, as well as φ-aromaticity in cyclic multinuclear metal complexes with f-electrons was also suggested [75]. And, a recent DFT study shows multiple σ-, π-, δ- and φ-aromaticity arising from U atom 5f orbital participation in the *cyclo*-U_3 cores of *cyclo*-U_3X_3 (X = O, NH) and *cyclo*-$U_3(\mu_2\text{-X})_3$ (X = C, CH, NH) [10,76].

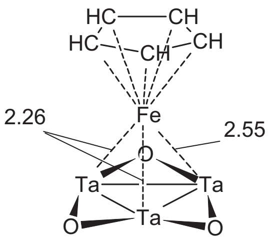

Fig. 6. Optimized structure of C_s symmetry calculated for $[\text{Ta}_3(\mu_2\text{-O})_3]\text{Fe}(\eta^5\text{-C}_5\text{H}_5)$ with the Fe–Ta bond distances in Å [77].

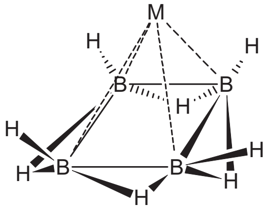

Fig. 7. Proposed structure of the η^4-B_4H_8 ring in $(\eta^4\text{-B}_4\text{H}_8)\text{Fe(CO)}_3$ [78] and $(\eta^4\text{-B}_4\text{H}_8)\text{Co}(\eta^5\text{-C}_5\text{H}_5)$ [79].

Another DFT study has shown the stability of the mainly ionic complexes $\text{M}[\text{Ta}_3(\mu_2\text{-O})_3]$ (M = Li, Na, K) (Fig. 2e) and $\text{M}[\text{Ta}_3(\mu_2\text{-O})_3]_2$ (M = Ca, Sr, Ba), with similar complexes of $[\text{M}_3(\mu_2\text{-O})_3]^-$ (M = Nb, V) also proposed as possible [77]. The optimized structure determined for $[\text{Ta}_3(\mu_2\text{-O})_3]\text{Fe}(\eta^5\text{-C}_5\text{H}_5)$ (Fig. 6) shows two strong Fe–Ta covalent bonds (2.26 Å) and one effective Fe–Ta interaction (2.55 Å).

3. *Cyclo*-X_4 ligands

3.1. Group 13 element rings

NMR (^{1}H and ^{11}B) data support a structure for the η^4-B_4H_8 rings in $(\eta^4\text{-B}_4\text{H}_8)\text{Fe(CO)}_3$ [78] and $(\eta^4\text{-B}_4\text{H}_8)\text{Co}(\eta^5\text{-C}_5\text{H}_5)$ with four terminal and four bridging H atoms (Fig. 7) [79].

The report of the first experimental and theoretical evidence for aromaticity in the all-metal *cyclo*-$Al_4{}^{2-}$ dianion found in the clusters $MAl_4{}^-$ (M = Li, Na, Cu) initiated research interest in aromaticity in other inorganic clusters and molecular systems [80]. Theoretical and gas phase photoelectron spectroscopic data for the *cyclo*-$X_4{}^{2-}$ dianions (X = B, Al [81], Ga, In, Tl) [21,82] and several of their mono and divalent metal cation salts [80,82–88] show that all but the Be^{2+}, Cu^{2+}, Zn^{2+} and Au^+ salts of the *cyclo*-$Al_4{}^{2-}$ dianion are ionic with planar, aromatic *cyclo*-$X_4{}^{2-}$ clusters and pyramidal structures

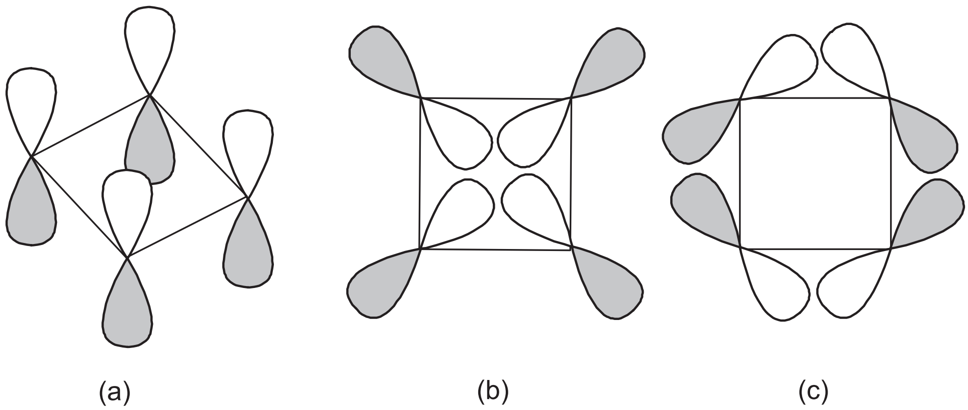
(a) (b) (c)

Fig. 8. The atomic p-orbital orientation that produces delocalized (a) π aromaticity and two types of σ ((b) radial and (c) tangential) aromaticity in $Al_4{}^{2-}$.

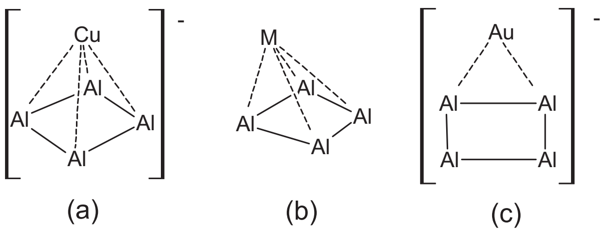

Fig. 9. Most stable structure for the clusters (a) $CuAl_4^-$ (C_{4v}) [86], (b) MAl_4 (M = Be, Zn) (C_s) [86] and (c) $AuAl_4^-$ (C_{2v}) [85].

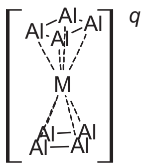

Fig. 10. Proposed structures for $[(\eta^4\text{-}Al_4)_2M]^q$ (M = Ti, Zr, Hf, q = 2-; M = V, Nb, Ta, q = 1-; M = Cr, Mo, W, q = 0) [92].

of C_{4v} symmetry. Since the ring-atom p orbitals produce one π- and two σ-delocalized aromatic bonds [84,89,90] (Fig. 8), it was concluded that both σ- and π-aromaticity should be included in bonding discussions for electron deficient all metal aromatic clusters [89,91].

The MAl_4 (M = Be, Zn) and $[CuAl_4]^-$ complexes, however, have largely covalent metal-ring bonds in which $[CuAl_4]^-$ has C_{4v} symmetry (Fig. 9a), while structures of C_s symmetry with two equivalent M–Al bonds, and the third and fourth longer and shorter than the two equivalent M–Al bonds is most stable for MAl_4 (M = Be, Zn) (Fig. 9b) [86]. A planar structure of C_{2v} symmetry is most stable for $AuAl_4^-$ (Fig. 9c) [85].

Calculations show that the double π- and σ-aromaticity of the square *cyclo*-Al_4^{2-} cluster is maintained on complex formation in $[(\eta^4\text{-}Al_4)_2M]^q$ (M = Ti, Zr, Hf, q = 2-; M = V, Nb, Ta, q = 1-; M = Cr, Mo, W, q = 0) and that the global minimum structures have D_{4d} symmetry with staggered *cyclo*-Al_4^{2-} units (Fig. 10) [92]. In addition the calculated NICS(0) and NICS(1) values (Table 3) show an increase in the σ-aromaticity and a decrease in the π-aromaticity of the *cyclo*-Al_4^{2-} cluster on complexation with the first-row transition elements, but a decrease in both π- and σ-aromaticity on complexation with the second- and third-row transition elements.

The $[Li_3Al_4]^-$ anion was first stabilized experimentally by Boldyrev, Wang and co-workers [90]. Their calculations show that the ground state structure of the Al_4^{4-} anion has a distorted rectangular shape (Fig. 11) with Al–Al bond lengths of 2.76, 2.58, 2.76 and 2.49 Å. Distortion from the perfect rectangular structure was attributed to the capping of the shortest Al–Al bond (2.49 Å) by one of the Li atoms.

Although there has been some disagreement, *cyclo*-Al_4^{4-} is generally considered to be antiaromatic [11,93]. Theoretical data show that *cyclo*-Al_4^{4-}, like *cyclo*-Al_4^{2-}, has one delocalized π- and two delocalized σ-molecular orbitals. However, the greater antiaromaticity arising from the 4 π-electrons compared to the aromaticity arising from the two filled σ-aromatic orbitals gives *cyclo*-Al_4^{4-} net antiaromatic character. This is consistent with the rectangular shape of *cyclo*-Al_4^{4-}, compared to the square shape of aromatic *cyclo*-Al_4^{2-} [21].

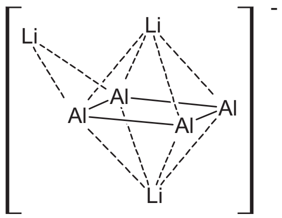

Fig. 11. Calculated ground state structure for the $[Li_3Al_4]^-$ anion at the CCSD(T)/6 311+G(2df) level [90].

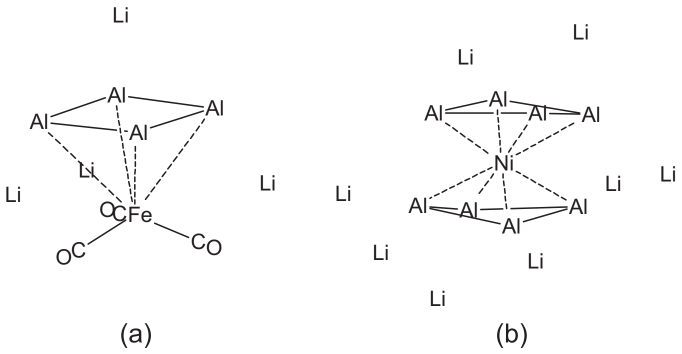

Fig. 12. Equilibrium minimum energy geometries for (a) $[(\eta^4\text{-}Al_4Li_4)]Fe(CO)_3$ and (b) $[(\eta^4\text{-}Al_4Li_4)]_2Ni$ [94].

Calculations show that *cyclo*-Al_4^{4-}, like antiaromatic 4 π-electron *cyclo*-C_4H_4, is stabilized in $[(\eta^4\text{-}Al_4M_4)]Fe(CO)_3$ (M = Li (Fig. 12a), Na, K) as an aromatic 6 π-electron ring [94]. And, while $[(\eta^4\text{-}Al_4Li_4)]Ni$ is unstable, $[(\eta^4\text{-}Al_4M_4)]_2Ni$ (M = Li (Fig. 12b), Na, K) are stable with the nonplanar *cyclo*-Al_4 atoms bent toward the Ni atom [94].

The thermodynamic instability of the $(Al_4Li_4)_2M$ (M = transition metal) complexes discussed above makes them susceptible to decomposition reactions and, as was also true for the *cyclo*-Al_3 cluster compounds discussed previously, the formation of energetically more stable fusion products [93]. DFT calculations show that the $[Al_4Li_3]^-$ cluster retains its antiaromaticity in $[DM(Al_4Li_3)]^q$ (M = Li, Na, K, q = 1-; Be, Mg, Ca, q = 0; D = $[Al_4Li_3]^-$, $\eta^5\text{-}C_5H_5^-$) due to electrostatic interactions [93], with the $\eta^5\text{-}C_5H_5^-$ ligand able to stabilize those complexes in which it is found.

3.2. Groups 13 and 14, 13 and 15 and 13 and 16 element rings

The M atoms in $[(\eta^5\text{-}C_5H_5)M(SiAl_3)]^q$ (M = Li, Na, K, q = 1-; M = Be, Mg, Ca, q = 0) prefer η^1-bonding with the Si atom or η^2-bonding

Table 3
NICS(0) and NICS(1) values (ppm) for the *cyclo*-Al_4^{2-} cluster as the free dianion and in the complexes $[(\eta^4\text{-}Al_4)_2M]^q$ (M = Ti, Zr, Hf, q = 2-; M = V, Nb, Ta, q = 1-; M = Cr, Mo, W, q = 0) computed at the B3LYP/6-311+G* level [92].

	Compounds									
	Al_4^{2-}	$[(\eta^4\text{-}Al_4)_2M]^{2-}$			$[(\eta^4\text{-}Al_4)_2M]^-$			$(\eta^4\text{-}Al_4)_2M$		
Metal atom (M):		Ti	Zr	Hf	V	Nb	Ta	Cr	Mo	W
Symmetry:	D_{4h}	D_{4d}	D_{4d}	D_{4d}	D_{4d}	C_1[a]	C_1[a]	C_1[a]	C_1[a]	C_1[a]
NICS(0)	−34.45	−36.86	−31.12	−25.49	−49.82	−27.41	−21.06	−37.08	−17.58	−13.26
NICS(1)	−27.38	−16.80	−18.54	−15.99	−17.03	−17.52	−14.56	−8.59	−14.92	−12.16

[a] A slight distortion from D_{4d} symmetry was required to remove some small imaginary vibration modes.

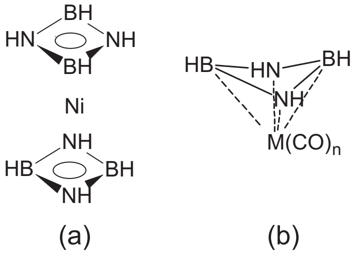

Fig. 13. The theoretical molecular structure of (a) $[\eta^4\text{-}(H_2B_2N_2H_2)]_2Ni$ [96] and (b) $[\eta^4\text{-}(H_2B_2N_2H_2)]M(CO)_n$ (M = Cr, n = 4; M = Fe, n = 3) [97].

with a side Al–Al bond rather than η^4-bonding to the center of the planar *cyclo*-$SiAl_3^-$ units [95]. The possible formation of extended oligomeric 1-D, 2-D or 3-D molecular structures or nanoscale forms was also suggested. Structurally they would contain alternating η^5-$C_5H_5^-$, M^{q+} and *cyclo*-$SiAl_3^-$ units, or *cyclo*-XAl_3^- (X = Ge, Sn, Pb) anions in place of the *cyclo*-$SiAl_3^-$ anions [95].

A theoretical study shows a structure of D_{2d} symmetry with eclipsed η^4-B_2N_2 rings (in which the B atoms in each ring face the N atoms in the other ring), rather than a structure of D_2 symmetry with staggered rings, or an eclipsed-ring structure of D_{2h} symmetry in which each B atom faces a B atom in the other ring, as most stable for $[\eta^4\text{-}(H_2B_2N_2H_2)]_2Ni$ (Fig. 13a) [96]. Some puckering of the η^4-B_2N_2 core, with the two B atoms of the *cyclo*-B_2N_2 core pointing away from the M atoms, has been proposed for $[\eta^4\text{-}(H_2B_2N_2H_2)]M(CO)_n$ (M = Cr, n = 4; M = Fe, n = 3) (Fig. 13b) [97]. An X-ray crystal study has confirmed ring-puckering in complexes with alkyl-substituted η^4-B_2N_2 rings [97].

Complexes have been prepared with transition metal carbonyl fragments bonded to the *cyclo*-B_2P_2 cores of $R_2B_2P_2R'_2$ (R and R′ = alkyl, (alkyl)$_2$N) and (aryl)$_2$N groups) ligands in a η^4 [5], η^3 (to the B_2P fragment) [98] and η^1 (to one or both B atoms) [99] manner. An X-ray crystal study shows that the *cyclo*-B_2P_2 core retains the planar, kite-shaped structure found in the free ligand on η^1-complexation in $[(Et_2N)_2B_2P_2(CMe_3)_2][Cr(CO)_5]_2$, while it becomes slightly folded in $[({}^iPr_2N)_2B_2P_2Et_2]Cr(CO)_5$ [99]. A complex with the Cr atom of the $Cr(CO)_5$ group η^1-bonded to the P atom of a *cyclo*-B_2NP core with mutually trans B atoms has also been reported [99].

Both experimental and theoretical molecular orbital and NICS data show that the molecules *cyclo*-Al_3X (X = As, Sb, Bi [100]) [101] have planar structures that, analogous to *cyclo*-Al_4^{2-}, have one delocalized π- and two delocalized σ-molecular orbitals. The similarity of the aromatic characteristics of these compounds to those of benzene has led to the proposal that they might possibly form metal sandwich complexes [100,101]. The credibility of this proposal is supported by the stability of the sandwich complexes of *cyclo*-Al_4^{2-} discussed above.

Calculations show that although complexation with d^6 transition metal atoms can stabilize the 6 π-electron *cyclo*-B_2S_2 ligand in $(B_2S_2)_2M$ (M = Cr, Mo, W), replacement of one of the two rings would produce the more stable complexes $(B_2S_2)M(CO)_3$ (M = Cr, Mo, W) and $(B_2S_2)Mn(\eta^5\text{-}C_5H_5)$ [102].

A theoretical analysis has been reported of the structures, stability and aromaticity of the $[Al_2P_2]^{2-}$ dianion, as well as of the salts $[M(Al_2P_2)]^-$ (M = Li, Na, K, Cu) and $[M(Al_2P_2)]$ (M = Be, Mg, Ca, Zn) [103]. The aromaticity of the $[Al_2P_2]^{2-}$ dianion is generally maintained in these salts.

3.3. Group 14 element rings

Similar to the Al_4^{2-} dianion, ab initio calculations show that the isovalence electronic Si_4^{2+} dication has a perfectly square-planar global minimum structure with both π- and doubly σ-aromatic character [104]. Adding two electrons to Si_4^{2+} produces the neutral σ-antiaromatic Si_4 cluster that has a rhombic distortion as the global minimum structure. The addition of four electrons to Si_4^{2+} produces the Si_4^{2-} dianion that was able to be studied experimentally using photoelectron spectroscopy once it was stabilized as $NaSi_4^-$ in the gas phase.

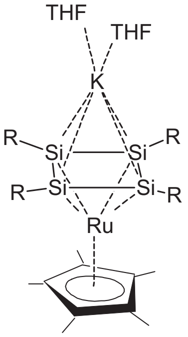

Fig. 14. X-ray crystal structure of $[K(THF)_2]^+[\{\eta^4({}^tBu_2MeSi)_4Si_4\}Co(\eta^5C_5Me_5)]^-$ (R = ${}^tBu_2MeSi$) [109].

X-ray data show a slight deviation from square-planar geometry of the *cyclo*-Si_4 core in $[\eta^4\text{-}({}^tBu_2MeSi)_4Si_4]M(CO)_3$ (M = Fe [105], Ru [106]) due to the staggered conformation of the CO ligands and the *cyclo*-Si_4 core produced by the steric effect of the ring substituents. Indeed, a more eclipsed configuration of the CO ligands and the Si_4 ring atoms, with less Si_4 ring distortion, is found in a theoretical study that replaced the ${}^tBu_2MeSi$ substituents with smaller Me_3Si groups [105,106]. X-ray data also show a slight deviation from square-planar geometry of the *cyclo*-Si_4 core in $[\eta^4\text{-}({}^tBu_2MeSi)_4Si_4]Co(\eta^5\text{-}C_5H_5)$ [107]. A slightly rectangular and nearly planar η^4-Si_4 ring with almost equal opposite Si–Si bond lengths is found in the K^+ ion salt of the $[\{\eta^4\text{-}({}^tBu_2MeSi)_4Si_4\}Co(CO)_2]^-$ anion due to partial delocalization of negative charge onto the ring [105,108]. The K^+ ion in this complex is bonded to an oxygen atom of one of the carbonyl groups. The K^+ ion also interacts in a η^4 manner in the anionic complex $[\{\eta^4\text{-}({}^tBu_2MeSi)_4Si_4\}Co(\eta^5\text{-}C_5Me_5)]^-$, as well with two THF molecules to produce a two-and-a-half layer sandwich structure (Fig. 14) [109]. Although the Si_4 ring in this complex is nearly square-planar, calculations of the optimized geometries for the complexes $[\{\eta^4\text{-}(RSi)_4Si_4\}Co(\eta^5\text{-}C_5Me_5)]^-$ (R = H_3Si, Me_3Si) show the Si_4 rings to be significantly folded and η^2-bonded to the Ru atom. The folding was attributed to the negative charge within these rings. The presence of a nearly planar Si_4 ring geometry in $[\{\eta^4\text{-}({}^tBu_2MeSi)_4Si_4\}Co(\eta^5\text{-}C_5Me_5)]^-$ was attributed to the neutralization of this electronic effect by a steric effect arising from a repulsive interaction between the large ${}^tBu_2MeSi$ groups on the Si_4 ring and the Me groups on the η^5-C_5Me_5 ring.

The presence of a *cyclo*-Si_3Ge core has been proposed in the synthesis of a complex formulated as $({}^tBu_2MeSi)_4Si_3Ge]Co(\eta^5\text{-}C_5H_5)$ [107].

3.4. Group 15 element rings

With 4 of 6 delocalized electrons in the highest occupied nonbonding π-orbital and the other 2 electrons contributing to aromatic stabilization, the *cyclo*-N_4^{2-} dianion is considered to be aromatic. In addition, NICS values show the presence of conflicting π-aromatic and σ-antiaromatic character (Table 4) [110]. Calculations show that the most stable structures for $[(\eta^4\text{-}N_4)_2M]^q$ (M = Ti, Fe, q = 2-; M = V, Co, q = 1-; M = Cr, Ni [111], q = 0) [110] have D_{4h} symmetry (with eclipsed rings) (Fig. 15a) for M = Ti, C_{2v} (or bent D_{4h}) symmetry for M = V and Cr, and D_{4d} symmetry (with staggered rings) (Fig. 15b) for M = Fe, Co and Ni. The low energy barrier

Table 4
NICS(0) and NICS(1) values (ppm) for *cyclo*-X_4^{2-} clusters (X = N [110], P [116]) as the free dianions and in the complexes with transition elements were computed at the B3LYP/6-311G level for X = N, and the B3LYP/6-311G* and B3LYP/6-311+G(2df,2dp) levels for X = P[a]. They were calculated at the B3LYP/6-311+G(d,p) level for the *cyclo*-Sb_4^{2-} dianion [26] and the B3LYP/LANL2DZ ECP level for the complexes of the *cyclo*-Sb_4^{2-} dianion with transition metals [123].

Compound	Symmetry	NICS(0)	NICS(1)
N_4^{2-}	D_{4h}	9.2	−4.19
$[(\eta^4\text{-}N_4)_2Ti]^{2-}$	D_{4h}	39.0	10.9
$[(\eta^4\text{-}N_4)_2V]^{-}$	C_{2v}[b]	64.9	17.3
$[(\eta^4\text{-}N_4)_2Cr]$	C_{2v}[b]	73.6	19.3
$[(\eta^4\text{-}N_4)_2Fe]^{2-}$	D_{4d}	−5.78	−16.80
$[(\eta^4\text{-}N_4)_2Co]^{-}$	D_{4d}	−5.45	−11.14
$[(\eta^4\text{-}N_4)_2Ni]$	D_{4d}	4.00	−3.00
P_4^{2-}	D_{4h}	8.63/5.96	1.97/2.41
$[(\eta^4\text{-}P_4)_2Ti]^{2-}$	D_{4h}	18.0/17.6	9.49/10.4
$[(\eta^4\text{-}P_4)_2V]^{-}$	D_{4h}	32.9/34.0	12.9/14.3
$[(\eta^4\text{-}P_4)_2Cr]^{2-}$	D_{4h}	44.4/52.0	18.5/21.8
$[(\eta^4\text{-}P_4)_2Mn]^{-}$	D_{4h}	94.5/105.3	33.1/37.1
$[(\eta^4\text{-}P_4)_2Fe]^{2-}$	D_{4d}	−4.78/−12.2	−0.07/−3.00
$[(\eta^4\text{-}P_4)_2Co]^{-}$	D_{4d}	−3.05/−9.30	0.20/−2.37
$[(\eta^4\text{-}P_4)_2Ni]$	D_{4d}	1.07/−5.15	0.80/−1.74
Sb_4^{2-}	D_{4h}	3.3	1.3
$[(\eta^4\text{-}Sb_4)_2Fe]^{2-}$	D_{4d}	−23.6	−10.8
$[(\eta^4\text{-}Sb_4)_2Ru]^{2-}$	D_{4d}	−9.13	−4.69
$[(\eta^4\text{-}Sb_4)_2Os]^{2-}$	D_{4d}	−8.43	−4.35
$[(\eta^4\text{-}Sb_4)_2Co]^{-}$	D_{4d}	−20.4	−10.1
$[(\eta^4\text{-}Sb_4)_2Rh]^{-}$	D_{4d}	−9.04	−4.28
$[(\eta^4\text{-}Sb_4)_2Ir]^{-}$	D_{4d}	−8.92	−3.99

[a] The first value is from a calculation at the B3LYP/6-311G* level and the second value is from a calculation at the B3LYP/6-311+G(2df,2dp) level.

[b] These compounds can also be viewed as having bent structures with D_{4d} symmetry.

between the D_{4h} and D_{4d} conformers calculated at the B3LYP/6-311+G* and BHLYP/6-311+G(3df,3pd) levels, however, led to the conclusion that there is probably no barrier to internal rotation of the two *cyclo*-N_4^{2-} ligands about the C_4 axis for $(\eta^4\text{-}N_4)_2Ni$ [111]. Although this complex can be considered as consisting of either two neutral 4 π-electron *cyclo*-N_4 ligands and a neutral Ni atom or, at the ionic limit, of two 6 π-electron *cyclo*-N_4^{2-} dianions and a Ni^{4+} cation, the latter structure was reported as more likely due to the calculated equivalence of the N–N bond lengths and bond indices of 1.2 that indicate the presence of delocalized rings [112].

The same study [112] compared the kinetic and structural stabilities of the possible reaction products of single nickel atoms with $(N_2)_n$ (n = 1–4). It was concluded that the end-on η^1-bound $Ni(N_2)_n$ (n = 1–4) complexes are preferred to the side-on η^2-bound and the N_4 bound complexes (that can be formulated as containing two side-on bound N_2 ligands), although the $Ni(N_2)_4$ complex with one *cyclo*-N_4 ligand and C_{2v} symmetry, and the $Ni(N_2)_4$ complex with two *cyclo*-N_4 ligands and D_{2d} symmetry may be kinetically stable.

NICS values (Table 4) show that on complex formation ring σ-antiaromaticity is enhanced and π-aromaticity destroyed in the Ti, V and Cr complexes, while ring σ- and π-aromaticity are both enhanced in the Fe and Co complexes, and the ring aromaticity does not change in the Ni complex. The *cyclo*-N_4^{2-} cluster in all complexes, even those characterized as antiaromatic, maintains a square geometry with equal N–N bond lengths. The feasibility of using *cyclo*-N_4^{2-} clusters to produce multi-decker structures was suggested, as was further condensation to form 1-D conducting polymers for possible use as semiconductors in nanostructure devices [110]. A more recent theoretical study concludes that several hetero-decker sandwich-like isomers $[N_3MN_5]^q$ are more thermodynamically stable than $[(\eta^4\text{-}N_4)_2M]^q$, with the $[(\eta^3\text{-}N_3)M(\eta^1\text{-}N_5)]^q$ and $[(\eta^3\text{-}N_3)M(\eta^2\text{-}N_5)]^q$ isomers ((M, q) = (Ni, 0), (Co, 1-), (Fe, 2-)) showing a high degree of kinetic stability that implies that they might exist at low temperatures [113]. In addition, based on the Natural Bond Orbital analysis of the $[(\eta^3\text{-}N_3)M(\eta^1\text{-}N_5)]^q$ and $[(\eta^3\text{-}N_3)M(\eta^2\text{-}N_5)]^q$ isomers ((M, q) = (Ni, 0), (Co, 1-), (Fe, 2-)), it was concluded that the N_3 unit is best represented as the triplet anion $^3N_3^-$, similar to that found in previously discussed *cyclo*-N_3 complexes [52].

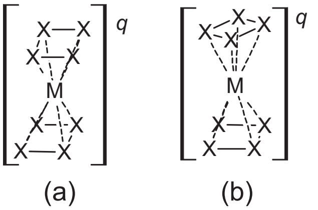

Fig. 15. The (a) eclipsed and (b) staggered conformations found for the *cyclo*-X_4^{2-} (X = N, P, Sb) ligands in transition metal complexes.

Using a combination of photoelectron spectroscopic data and theoretical calculations, it has been concluded that the X_4^{2-} dianions present in $Na^+X_4^{2-}$ (X = P, As, Sb) have perfectly square-planar global minimum structures [114].

One of the 152 species produced in the laser ablation of solid CoP has been characterized as $[CoP_8]^-$ [115]. This study also concluded that the most stable structure contains two planar η^4-P_4 clusters that are bonded to the Co atom in a parallel and staggered D_{4d} conformation (Fig. 15b). In a more recent theoretical study it was concluded that while the staggered ring conformation is most stable for $[(\eta^4\text{-}P_4)_2M]^q$ ((M, q) = (Cr, 2-); (Mn, 1-), (Fe, 2-), (Co, 1-), (Ni, 0)), the D_{4h} structure with parallel and eclipsed rings (Fig. 15a) is most stable for $[(\eta^4\text{-}P_4)_2M]^q$ ((M, q) = (Ti, 2-); (V, 1-)) [116]. In addition, calculated NICS values (Table 4) show that the rings in the Ti, V, Cr and Mn complexes are σ- and π-antiaromatic. With the exception of the small positive NICS(0) value for the Ni complex calculated at the B3LYP/6-311G* level, the other NICS(0) values are negative for the Fe, Co and Ni complexes calculated at both the B3LYP/6-311G* and B3LYP/6-311+G(2df,2dp) levels. In addition, the NICS(1) values are very slightly negative for the Fe complex and slightly positive for the Co and Ni complexes when calculated at the B3LYP/6-311G* level, but marginally negative for all three complexes at the B3LYP/6-311+G(2df,2dp) level. Since the values calculated at the B3LYP/6-311+G(2df,2dp) level were considered to be more reasonable in that they included a larger basis set, it was concluded that the Fe, Co and Ni complexes are σ- and π-aromatic [116]. The conclusion that the *cyclo*-P_4^{2-} complexes of the early first-row transition metals Ti, V and Cr are antiaromatic, while those of the later first-row transition elements Fe, Co and Ni are aromatic, is similar to findings for the analogous *cyclo*-N_4^{2-} ligand complexes discussed previously [110].

Since, with the possible exception of $[CoP_8]^-$, *cyclo*-P_4^{2-} complexes of the first-row transition elements have not been synthesized, experimental structural data are unavailable for comparison with the theoretical predictions. However, some *cyclo*-P_4^{2-} complexes of the second- and third-row transition elements have been reported and characterized using X-ray crystallography. Data for $(\eta^5\text{-}C_5Me_5)Nb(CO)_2(\eta^4\text{-}P_4)$ (Fig. 16) have been interpreted as showing either an allyl-like *cyclo*-P_4^{2-} unit (with a $4d^2$ Nb electron configuration) or a neutral antiaromatic 4 π-electron *cyclo*-P_4 unit (with a $4d^4$ Nb electron configuration) in which the coplanar ring P atoms form a kite-shaped or slightly distorted square with two adjacent longer (2.181(2) and 2.178(2) Å) and two adjacent shorter (2.136(2) and 2.141(2) Å) P–P bond lengths [117].

The *cyclo*-P_4 unit has a similar structure in the complex $[\eta^5\text{-}(1,3\text{-}^tBu_2C_5H_3)][Ta(CO)_2(\eta^4\text{-}P_4)]$ (adjacent longer P–P distances = 2.172(3) and 2.173(3) Å; adjacent shorter P–P distances = 2.150(3) and 2.155(2) Å) [118]. One X-ray crystal study shows a similar structure for the *cyclo*-P_4 unit in the W complex

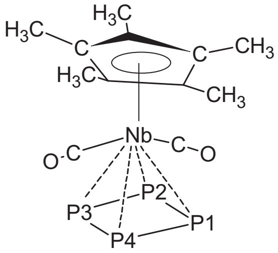

Fig. 16. X-ray crystal structure of $(\eta^5\text{-}C_5Me_5)Nb(CO)_2(\eta^4\text{-}P_4)$ [117]. The P–P bond distances in units of Å are: P1–P2 = 2.136(2), P2–P3 = 2.141(2), P3–P4 = 2.181(2) and P4–P1 = 2.178(2). The P–P–P bond angles in deg are: P1–P2–P3 = 92.6(1), P2–P3–P4 = 88.4(1), P3–P4–P1 = 90.4(1), P4–P1–P2 = 88.6(1).

of the $[(\eta^4\text{-}P_4)M(CO)_4][(M(CO)_5]_4$ (M = Cr, W) series [119], while another study of the W complex that included X-ray and ^{31}P NMR data concluded that the planar, kite-shaped *cyclo*-P_4 ligand might formally be represented as *cyclo*-$P_4{}^{2-}$ and described as consisting of an allylic-like $P_3{}^-$ anion coordinated to a P^- anion [120]. Breaking one of the four P-W(CO)$_5$ bonds in $[(\eta^4\text{-}P_4)W(CO)_4][(W(CO)_5]_4$ produced a butterfly-shaped *cyclo*-P_4 ligand that is η^3-bonded to the W atom of a $(CH_3CN)_2(CO)_2WCl$ unit [121].

Only one complex containing a *cyclo*-As_4 ligand has been synthesized. It consists of a nearly square and neutral *cyclo*-As_4 unit that is bridged by two Co containing fragments (Fig. 17) in the triple-decker sandwich compound $[\{\eta^5\text{-}(C_5H_4{}^tBu)Co\}_2\{\mu\text{-}(\eta^4{:}\eta^4\text{-}As_4)\}][Co_3Cl_8(THF)_2]$ [122].

Theoretical data, including calculated equilibrium geometries and NICS values, have been reported for $[(\eta^4\text{-}Sb_4)_2M]^q$ (M = Fe, Ru, Os, q = 2-; M = Co, Rh, Ir, q = 1-) [123]. The square structure of the *cyclo*-$Sb_4{}^{2-}$ ligand remains unchanged on complex formation to give complexes with D_{4d} symmetry in which the parallel rings take on the staggered conformation (Fig. 15b). The NICS data for these complexes (Table 4) show that the *cyclo*-$Sb_4{}^{2-}$ ligands exhibit σ- and π-aromaticity. The addition of Na^+ can stabilize the complexes as $[Na(\eta^4\text{-}Sb_4)_2M]^-$ (M = Fe, Ru, Os) and prevent them from undergoing electron detachment.

3.5. Group 16 element rings

The ability of *cyclo*-$X_4{}^{2+}$ (X = S, Se) dications to form 6 π-electron complexes with transition metal carbonyls has been investigated theoretically [124]. The syntheses and structures have been reported for the $Br_6{}^{6-}$ [125] and $I_6{}^{6-}$ [126] salts of the binuclear Mo(III) complex formulated as $[Mo_2(\eta^2\text{-}Te_2)_2(\eta^4\text{-}Te_4)_2]^{6+}$ (Fig. 17). The pair of Mo(III) atoms is bridged by the two η^2-$Te_2{}^{2+}$ dications. Each Mo(III) atom is also bonded to a terminal η^4-$Te_4{}^{2+}$ ring that has a butterfly conformation rather than the planar structure of D_{4h} symmetry found for the free $Te_4{}^{2+}$ dication [126].

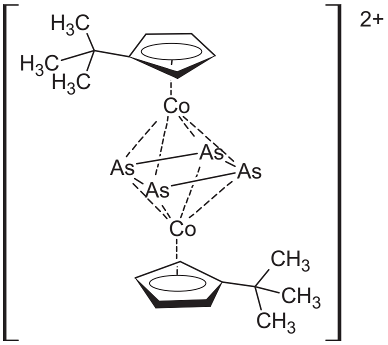

Fig. 17. X-ray crystal structure reported for the $[\{\eta^5\text{-}(C_5H_4{}^tBu)Co\}_2\{\mu\text{-}(\eta^4{:}\eta^4\text{-}As_4)\}]^{2+}$ dication in $[\{\eta^5\text{-}(C_5H_4{}^tBu)Co\}_2\{\mu\text{-}(\eta^4{:}\eta^4\text{-}As_4)\}][Co_3Cl_8(THF)_2]$ [122].

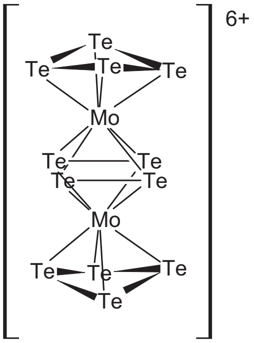

Fig. 18. X-ray crystal structure of the $[Mo_2(\eta^2\text{-}Te_2)_2(\eta^4\text{-}Te_4)_2]^{6+}$ cation [126].

The wings of the η^4-$Te_4{}^{2+}$ rings point toward the Mo(III) atoms. Although the short distance found between the two Mo(III) atoms (297.16(5) pm) seems to indicate the presence of a chemical bond, coupling of the magnetic moments is not observed, and a paramagnetic moment of 3.53μ_B per Mo(III) atom corresponds to the presence of a diradical with 17 valence electrons for each Mo(III) atom [126] (Fig. 18).

3.6. f-block element rings

A recent DFT study has shown multiple σ-, π-, δ- and φ-aromaticity arising from U atom 5f orbital participation in the *cyclo*-U_4 cores of *cyclo*-U_4X_4 (X = O, NH) and *cyclo*-$U_4(\mu_2\text{-}X)_4$ (X = C, CH, NH) [10,76]. The *cyclo*-U_4 core of *cyclo*-$U_4(\mu_2\text{-}C)_4$ is able to accommodate a Si atom to form a thermodynamically stable and coplanar complex (Fig. 19a) and retain to some extent its aromaticity. However, it is too small to accommodate the larger Ge atom that interacts more weakly and caps a ring face at a distance of 1.125 Å above the ring centroid (Fig. 19b).

4. *Cyclo*-X_5 ligands

4.1. Group 13 element rings

A single crystal X-ray study of $[(\eta^5\text{-}C_5Me_5)ReH]_2[\mu\text{-}(\eta^5{:}\eta^5\text{-}B_5Cl_5)]$ (Fig. 20) shows the *cyclo*-B_5Cl_5 ligand to be planar, but did not allow for the location of the H atoms in the Re–H bonds [127]. The ^{11}B NMR spectrum of this compound shows three signals with an intensity ratio of 2:2:1 and no large coupling with the protons.

4.2. Groups 13 and 15 element rings

Calculations in one study show a preferred structure with eclipsed η^5-rings in $[\eta^5\text{-}\{(BR)_2(N_3R')_2\}]_2Fe$ (R = CH_3, R′ = C_6H_5) [128]. The complex was also described as containing 20 valence electrons. A more recent study concludes that the staggered

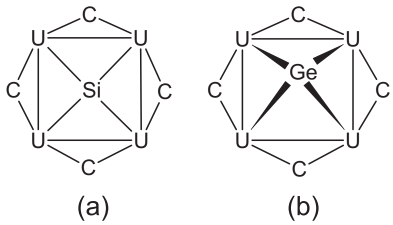

Fig. 19. Calculated equilibrium structures of the (a) planar Si@[*cyclo*-$U_4(\mu_2\text{-}C)_4$] molecule with D_{4h} symmetry and of the (b) pyramidal Ge@[*cyclo*-$U_4(\mu_2\text{-}C)_4$] molecule with C_{4v} symmetry [76].

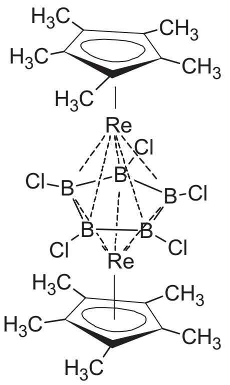

Fig. 20. X-ray crystal structure for $[(\eta^5\text{-}C_5Me_5)ReH]_2[\mu\text{-}(\eta^5{:}\eta^5\text{-}B_5Cl_5)]$ [127].

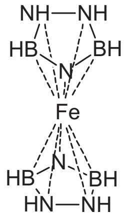

Fig. 21. Theoretical structure proposed for $[\{\eta^5\text{-}(B_2H_2)(N_3H_2)\}]_2Fe$ [97].

η^5-ring conformation is most stable in the related complex $[\eta^5\text{-}\{(B_2H_2)(N_3H_2)\}]_2Fe$ (Fig. 21) and that this complex has 18 rather than 20 valence electrons [97].

4.3. Group 14 element rings

Although the $S_5H_5^-$ anion has a nonplanar puckered global minimum structure due to the pseudo-Jahn–Teller effect, a theoretical study has shown that this effect can be suppressed through coordination with two Mg^{2+} cations to form the inverse sandwich complex $Mg^{2+}Si_5H_5^-Mg^{2+}$ (Fig. 22) [129]. The $S_5H_5^-$ anion in this complex is aromatic and planar, although calculated $NICS_{zz}$ values show it to be less aromatic than the $C_5H_5^-$ anion. The presence of two Li^+, Na^+ or Be^{2+} cations, however, rather than the two Mg^{2+} cations, does not completely suppress the pseudo-Jahn–Teller effect.

A theoretical study has shown that both $(\eta^5\text{-}Si_5H_5)_2Fe$ and $(\eta^5\text{-}C_5H_5)_2Fe$ are stable as the staggered D_{5d} conformer, and that the Fe atom is more cationic and interacts more strongly with the ring in $(\eta^5\text{-}C_5H_5)_2Fe$ than in $(\eta^5\text{-}Si_5H_5)_2Fe$ [130].

A planar *cyclo*-Pb_5^{4-} anion covalently bridges the two $Mo(CO)_3$ units in $[\{Mo(CO)_3\}_2\{\mu\text{-}(\eta^5{:}\eta^5\text{-}Pb_5)\}]^{4-}$ (Fig. 23) [131] with a relatively large donation of charge from the *cyclo*-Pb_5^{4-} to the $Mo(CO)_3$ units. Donation of only one electron from *cyclo*-Pb_5^{4-} to each $Mo(CO)_3$ unit would change it from an antiaromatic 4 π-electron to an aromatic 2 π-electron ligand.

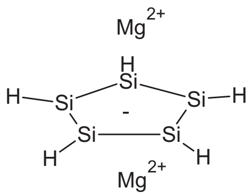

Fig. 22. Optimized $^1A_1'$ ground state structure with D_{5h} symmetry determined for $Mg^{2+}Si_5H_5^-Mg^{2+}$ [129].

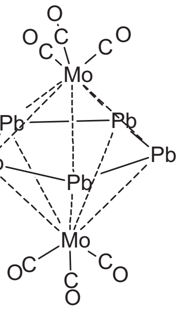

Fig. 23. X-ray crystal structure of $[\{Mo(CO)_3\}_2\{\mu\text{-}(\eta^5{:}\eta^5\text{-}Pb_5)\}]^{4-}$ [131].

4.4. Group 15 element rings

Both photoelectron spectroscopic data and ab initio calculations show that the X_5^- (X = P, As, Sb, Bi) anions have a cyclic aromatic ground state structure with D_{5h} symmetry [132]. Calculations show that although a pyramidal half-sandwich structure of C_{5v} symmetry is most stable for the aromatic compounds $[X_5Fe]^+$ (X = N, P, As), a planar structure of D_{5h} symmetry is most stable for $[X_5Fe]^+$ (X = Sb, Bi) [133]. While these calculations show that $[X_5Fe]^+$ (X = Sb, Bi) are in the singlet ($^1A_1'$) electronic ground state, preliminary calculations have shown that for the triplet ($^3A''$) electronic state, a slightly pyramidal structure of C_s symmetry is most stable for $[X_5Fe]^+$ (X = Sb, Bi) [133]. The Fe-ring bonding is slightly more covalent than electrostatic. The calculations were performed by choosing an interaction between neutral Fe atoms and *cyclo*-X_5^+ (X = Sb, Bi) units with 6 π-electrons rather than Fe^{2+} ions and X_5^- (X = Sb, Bi) units since the latter species pair has a much higher charge separation [133].

Calculations have been used to analyze and compare changes in the bonding in $(\eta^5\text{-}C_5H_5)_2Fe$ as the C–H fragments of one of the two cyclopentadienyl rings are replaced by N atoms to produce $(\eta^5\text{-}C_5H_5)FeN_5$, and by P atoms to produce $(\eta^5\text{-}C_5H_5)FeP_5$ [134]. For the azaferrocenes, the process results in the Fe atom becoming more positive and the substituted ring becoming more negative, while for the phosphaferrocenes, both the Fe and the substituted ring became more negative. In addition, since the η^5-bonding mode is preferred in complexes containing the P-substituted ring, it was concluded [102] that the recently proposed [135] synthesis of a η^5-N_5 complex without the protection of the N lone pairs will be difficult due to the preference of these rings for η^1-bonding.

Indeed, other theoretical data show a variety of stable ring bonding modes for aromatic *cyclo*-N_5^- ligands (Fig. 24) in $(\eta^n\text{-}N_5)_2M$ (n = 5, M = Ti [136], V, Cr, Fe [135,137], Co) [138]; n = 3, M = Ni [138]; n = 2, M = Mn [138]; n = 1, M = Zn [139]). However, only the η^5-bonding mode is stable for *cyclo*-P_5^- ligands in $(\eta^5\text{-}P_5)_2M$ (M = Ti [137], Fe [136,140], Ru [140], Os [140]), *cyclo*-As_5^- ligands in $(\eta^5\text{-}As_5)_2M$ (M = Ti [137], Fe [136]), *cyclo*-Sb_5^- ligands in $(\eta^5\text{-}Sb_5)_2M$ (M = Ti [137], Fe [133,136]) and the *cyclo*-Bi_5^- ligand in $(\eta^5\text{-}Bi_5)_2Fe$ [133]. While the complexed rings maintain 56–68%

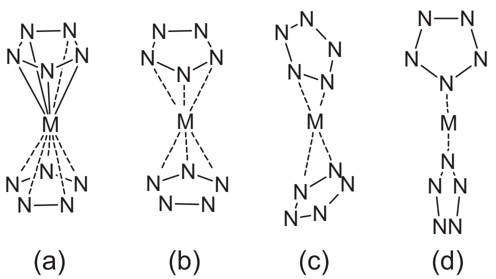

Fig. 24. The (a) η^5, (b) η^3, (c) η^2 and (d) η^1 structures found for *cyclo*-N_5^- ligands in $(N_5)_2M$ complexes of the first-row transition elements.

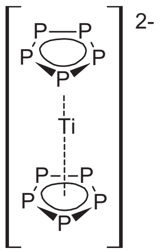

Fig. 25. X-ray crystal structure found for $[(\eta^5\text{-}P_5)_2Ti]^{2-}$ as the tetraphenylphosphonium and bis(triphenylphosphonium)iminium salts [141].

of their aromatic character in $(\eta^5\text{-}C_5H_5)_2Fe$ relative to the free rings, only 26–51% is maintained for the rings in $(\eta^5\text{-}P_5)_2Fe$ [140].

Approximately 50 years after the reported synthesis of ferrocene [32,33], Schleyer and co-workers reported the synthesis and structural characterization of the first carbon-free inorganic metallocene sandwich complex $[(\eta^5\text{-}P_5)_2Ti]^{2-}$ [141]. The solid-state D_{5h} symmetry structure of $[(\eta^5\text{-}P_5)_2Ti]^{2-}$ (Fig. 25) shows two parallel and eclipsed aromatic $\eta^5\text{-}P_5^-$ rings with an average P–P bond length of 2.154(9) Å, which is between the values expected for P–P single and P=P double bonds [141]. A theoretical study of *cyclo*-P_5^-, $[(\eta^5\text{-}P_5)Ti]^-$ and $[(\eta^5\text{-}P_5)_2Ti]^{2-}$ [142] also shows equal P–P distances for the five coplanar P atoms of each *cyclo*-P_5^- unit, with a distance of 2.175 Å calculated for ring P–P bonds of the isolated $[(\eta^5\text{-}P_5)_2Ti]^{2-}$ dianion with D_{5h} symmetry. The gas phase decomposition of $[NbAs_8]^{3-}$ was reported to produce the K^+ salt of $[NbAs_{10}]^{3-}$, which is a possible analogue of $[(\eta^5\text{-}P_5)_2Ti]^{2-}$ [143].

Other transition metal complexes have been synthesized with both $\eta^5\text{-}X_5^-$ (X = P, As) [60] and $[\mu\text{-}(\eta^5{:}\eta^5\text{-}X_5)]^-$ (X = P [59], As [59,60,144], Sb [145]) rings. Calculations show that the eclipsed structure of D_{5h} symmetry is the minimum on the potential energy surface for $[(\eta^5\text{-}C_5H_5)Fe]_2[\mu\text{-}(\eta^5{:}\eta^5\text{-}X_5)]$ (X = CH, P, As) [146]. They also show that the $\mu\text{-}(\eta^5{:}\eta^5\text{-}X_5)$ (X = P, As) rings expand significantly due to a loss of π-electron density that is directed to bonding with the two Fe centers and that gives the Fe atoms a negative charge. Molecular orbital calculations have been used to explain the presence of an undistorted planar $\mu\text{-}(\eta^5{:}\eta^5\text{-}P_5)$ ring in $[(\eta^5\text{-}C_5Me_5)Cr]_2[\mu\text{-}(\eta^5{:}\eta^5\text{-}P_5)]$ but a distorted planar $\mu\text{-}(\eta^4{:}\eta^4\text{-}As_5)$ ring in $[(\eta^5\text{-}C_5H_5)Mo]_2[\mu\text{-}(\eta^4{:}\eta^4\text{-}As_5)]$ that was further characterized as consisting of As_2 and allylic As_3 subunits [147]. These calculations show that the greater energy range of the *cyclo*-P_5 orbitals (60 eV) relative to the *cyclo*-As_5 orbitals (15 eV) produces a non-degenerate ground state for $[(\eta^5\text{-}C_5Me_5)Cr]_2[\mu\text{-}(\eta^5{:}\eta^5\text{-}P_5)]$ and a degenerate ground state for $[(\eta^5\text{-}C_5H_5)Mo]_2[\mu\text{-}(\eta^4{:}\eta^4\text{-}As_5)]$. As a result, a Jahn–Teller distortion was predicted in the As_5 ring, and, by implication, an even greater distortion was expected in Sb_5 ring complexes [147]. However, since these reported molecular orbital studies, little ring distortion has been observed in complexes with $\mu\text{-}(\eta^5{:}\eta^5\text{-}X_5)$ rings (X = As [148], Sb [145]). And, based on the presence of a small distortion in the $\mu\text{-}(\eta^5{:}\eta^5\text{-}Sb_5)$ ring in $[\{\eta^5\text{-}(1,2,4\text{-}{}^tBu_3C_5H_2)\}Mo][\mu\text{-}(\eta^5{:}\eta^5\text{-}Sb_5)][\{\eta^5\text{-}(1,4\text{-}{}^tBu_2\text{-}2\text{-}MeC_5H_2)\}Mo]$, it was concluded that the distortion of the $\mu\text{-}(\eta^4{:}\eta^4\text{-}As_5)$ ring in $[(\eta^5\text{-}C_5H_5)Mo]_2[\mu\text{-}(\eta^4{:}\eta^4\text{-}As_5)]$ is due to strong intermolecular interactions and not to the Jahn–Teller effect [145].

The X-ray structure of the inverse sandwich complex $[\{(\eta^5\text{-}C_5H_5)Cr(CO)_2\}_2(\mu\text{-}PH)]$ $[\{(\eta^5\text{-}C_5H_5)Cr\}_2\{\mu\text{-}(\eta^1{:}\eta^1{:}\eta^5{:}\eta^5\text{-}P_5)\}]$ shows a pseudo-*cyclo*-P_5 ring that appears to consist of P_2 and allylic P_3 subunits (Fig. 26a) [149]. Two adjacent P atoms of the ring are η^1-bonded to two additional Cr atoms of a fragment in which the Cr atoms are also linked by the P atom of a PH group. Another inverse sandwich compound, $[\{(\eta^5\text{-}C_5H_5)Cr(CO)\}(\eta^3\text{-}P_3)][\{(\eta^5\text{-}C_5H_5)Cr\}_2\{\mu\text{-}(\eta^1{:}\eta^5{:}\eta^5\text{-}P_5)\}]$ (Fig. 26b) has two Cr atoms that are η^5-bonded to either side of a distorted bridging *cyclo*-P_5^- unit that is also η^1-bonded to a third Cr atom of a $[(\eta^5\text{-}C_5H_5)Cr(CO)](\eta^3\text{-}P_3)$ fragment [150].

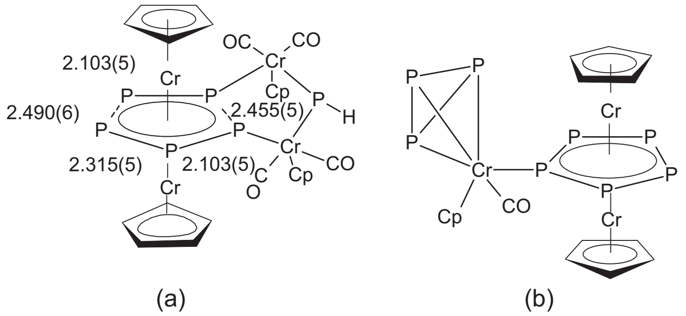

Fig. 26. X-ray crystal structure determined for (a) $[\{(\eta^5\text{-}C_5H_5)Cr(CO)_2\}_2(\mu\text{-}PH)]$ $[\{(\eta^5\text{-}C_5H_5)Cr\}_2\{\mu\text{-}(\eta^1{:}\eta^1{:}\eta^5{:}\eta^5\text{-}P_5)\}]$ in which the numbers represent P–P bond lengths given in Å units [149] and (b) $[\{(\eta^5\text{-}C_5H_5)Cr(CO)\}(\eta^3\text{-}P_3)][\{(\eta^5\text{-}C_5H_5)Cr\}_2\{\mu\text{-}(\eta^1{:}\eta^5{:}\eta^5\text{-}P_5)\}]$ [150].

Although no signals were observed in the EPR (130 K) and ^{31}P (300 K) spectra, the fragmentation pattern in the mass spectrum of a brown solid isolated from toluene has been interpreted as showing the presence of a mixture of the inverse sandwich compounds $[(\eta^5\text{-}C_5H_5)Cr]_2[\mu\text{-}(\eta^5{:}\eta^5\text{-}P_nAs_{5-n})]$ (n = 1–5) [56].

4.5. f-block element rings

A DFT study has shown multiple σ-, π-, δ- and φ-aromaticity arising from U atom 5f orbital participation in the *cyclo*-U_5 core of *cyclo*-$U_5(\mu_2\text{-}C)_5$ [10,76]. The *cyclo*-U_5 core of *cyclo*-$U_5(\mu_2\text{-}C)_5$ is large enough to accommodate a sixth U atom in the thermodynamically stable and coplanar complex U@[*cyclo*-$U_5(\mu_2\text{-}C)_5$] (Fig. 27) that retains to some extent its aromaticity.

5. *Cyclo*-X_6 ligands

5.1. Group 13 element rings

Calculations show the stability of the C_{6v} symmetry sandwich complexes $[(\eta^6\text{-}CB_6)M]^q$ ((M, q) = (Mn, 1-), (Fe, 0), (Co, 1+)), D_{6d} symmetry sandwich complexes $[(\eta^6\text{-}XB_6)_2M]^q$ (X = C, M = Fe, Co, Ni, q = 2-, 1-, 0, respectively; X = N, M = Fe, Mn, q = 0, 1-, respectively) (Fig. 28) [151], triple-decker complexes $[(\eta^n\text{-}C_nH_n)M]_2[\{\mu\text{-}(\eta^6{:}\eta^6\text{-}XB_6)\}]$ (X = B, C, N; M = Mn, Fe, Ru, Re; n = 5, 6) [152] and tetra-decker complexes $(\eta^5\text{-}C_5H_5)Fe[\{\mu\text{-}(\eta^6{:}\eta^6\text{-}XB_6)\}]Fe[\{\mu\text{-}(\eta^6{:}\eta^6\text{-}XB_6)\}]Fe(\eta^5\text{-}C_5H_5)$ (X = B, C) [153].

It was suggested that the Fe centers in the tetra-decker complexes can be replaced with Ru, Os or other transition metals and that the stabilizing ability of $[(\eta^5\text{-}C_5H_5)Fe]^+$ cations might allow expansion of the tetra-decker complexes to contain more than two $(\eta^6\text{-}XB_6)Fe$ (X = B, C) units [153]. Since studies of transition metal complexes of the hypercarbon $[CB_6]^{2-}$ dianion [151] have not considered the possible fusion of two $[CB_6]^{2-}$ clusters, the difficulty [154] and therefore feasibility [155] of the synthetic procedure proposed has been questioned. It has also been proposed [155] that the $[CB_6]^{2-}$ dianion can be stabilized with the $\eta^5\text{-}C_5H_5^-$ ligand in the

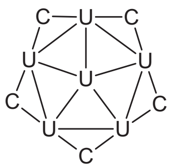

Fig. 27. Computed equilibrium geometry of the planar U@[*cyclo*-$U_5(\mu_2\text{-}C)_5$] molecule with D_{5h} symmetry [76].

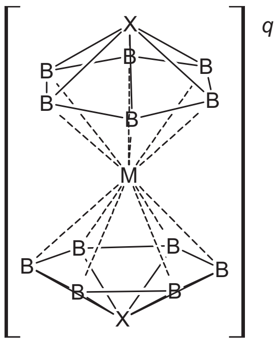

Fig. 28. Structures of D_{6d} symmetry proposed for $[(\eta^6\text{-}XB_6)_2M]^q$ (X = C, M = Fe, Co, Ni, q = 2-, 1-, 0, respectively; X = N, M = Fe, Mn, q = 0, 1-, respectively) [151].

hetero-decker complexes $(\eta^5\text{-}C_5H_5)M(CB_6)^q$ (M = Li, Na, K, q = 2-; Be, Mg, Ca, q = 1-) and that other complexes with metals including Cu^+, Ag^+ and Au^+, or planar and capped hypercoordinate aromatic molecules including $[NB_6]^-$ and $B_7{}^-$, might be synthesized.

However, since these theoretical studies of transition metal complexes of the $[CB_6]^{2-}$ cluster have appeared, analyses that use both photoelectron spectroscopic data and ab initio calculations have shown that the global minimum structure of the $[CB_6]^{2-}$ dianion, and its isoelectronic analogues $[C_2B_5]^{2-}$ and $[CB_6]^-$, is not planar and does not possess a hexacoordinate C atom [16,17]. Rather, with C being more electronegative than B, it prefers peripheral positions where it is better able to form σ-type two-center two-electron bonds [17]. It was further concluded that since the planar carbon-centered planar isomers have such high energies, it is not possible to produce these compounds experimentally.

A DFT study has suggested the presence of the *cyclo*-B_6H_6 ligand in $[(\eta^6\text{-}C_6H_6)Mo]_2[\mu\text{-}(\eta^6\text{:}\eta^6\text{-}B_6H_6)]$ [156]. Another theoretical study compares the transformation of $[(\eta^5\text{-}C_5H_5)Re]_2[\mu\text{-}(\eta^6\text{:}\eta^6\text{-}B_6H_6)]$ into $[(\eta^5\text{-}C_5H_5)Re]_2(B_5H_7)$ and $[(\eta^5\text{-}C_5H_5)W]_2(B_5H_9)$ [157]. Both NMR (^{11}B and ^{1}H) and X-ray data show a planar *cyclo*-B_6 unit in the 24 valence electron complex $[(\eta^5\text{-}C_5Me_5)Re]_2[\mu\text{-}\{\eta^6\text{:}\eta^6\text{-}(1,2\text{-}B_6H_4Cl_2)\}]$ (Fig. 29). This contrasts with the puckered *cyclo*-P_6 unit found in 24 valence electron complexes noted below [127,158].

An inverse sandwich complex with a unique aromatic, inorganic benzene analogue B_4Co_2 ring of a $B_4Co_2H_4$ unit sandwiched between two $(\eta^5\text{-}C_5Me_5)$Re groups (Fig. 30) has been synthesized and characterized using X-ray crystallography [159].

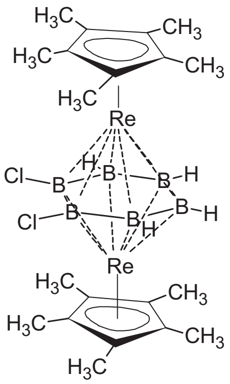

Fig. 29. X-ray crystal structure for $[(\eta^5\text{-}C_5Me_5)Re]_2[\mu\text{-}\{\eta^6\text{:}\eta^6\text{-}(1,2\text{-}B_6H_4Cl_2)\}]$ [127,158].

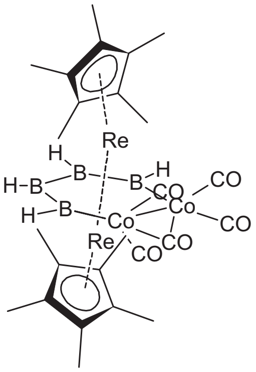

Fig. 30. X-ray crystal structure of $[(\eta^5\text{-}C_5Me_5)Re]_2[\mu\text{-}\{\eta^6\text{:}\eta^6\text{-}B_4H_4Co_2(CO)_5\}]$ that contains an inorganic benzene analogue B_4Co_2 ring [159].

5.2. Groups 13 and 15 element rings

Various conclusions have been reached concerning the extent to which "inorganic benzenes" such as borazine, *cyclo*-$B_3N_3H_6$ (Fig. 1), are aromatic [30,160–172]. This illustrates how the use of different criteria can sometimes lead to different conclusions concerning the presence of molecular aromaticity. One recent study, however, has concluded that the present general view is that borazine is either nonaromatic or possibly only slightly aromatic [172]. As another example of this discrepancy, while theoretical aromatic stabilization energy calculations show that borazine and its phosphorus analogue *cyclo*-$B_3P_3H_6$ are equally aromatic, magnetic susceptibility and NICS data show that *cyclo*-$B_3N_3H_6$ is not while *cyclo*-$B_3P_3H_6$ is aromatic [162,166]. Likewise, the nature of the metal-ring interaction in $Cr(CO)_3$ complexes of these rings can either be described as η^3 and triamine with the Cr atom interacting with the three nitrogen atom lone electron pairs of a puckered ring (Fig. 31a), or as η^6 with the Cr atom interacting with a planar delocalized ring (Fig. 31b). One theoretical study has concluded that greater predicted puckering of the *cyclo*-B_3X_3 core in $(B_3N_3H_6)Cr(CO)_3$ than in $(B_3P_3H_6)Cr(CO)_3$ indicates less ring π-delocalization and greater σ-bonding between the Cr and N atoms than between the Cr and P atoms [162]. Although another theoretical study of $(B_3N_3H_6)Cr(CO)_3$ again predicts a puckered *cyclo*-B_3N_3 core with shorter Cr–N than Cr–B bonds, it was further concluded that the ring should still be considered delocalized rather than acting as a triamine ligand [173]. For comparison, X-ray crystal data show a delocalized but puckered *cyclo*-B_3N_3 core in $[(C_2H_5)_3B_3N_3(C_2H_5)_3]Cr(CO)_3$ [174], and a similar puckered but almost planar *cyclo*-B_3P_3 core in $[(\text{mesityl})_3B_3P_3(C_6H_5)_3]Cr(CO)_3$ [175].

DFT studies have been reported for 1-D crystals or nanowires formed by multidecker sandwich complexes of the early first-row transition elements and borazine due to the expectation that these materials will exhibit interesting electronic structures. The relatively small $V_n(B_3N_3H_6)_{n+1}$ (n = 1–4) clusters were structurally more stable than analogues in which the benzene molecule replaces the borazine ring, while the infinite 1-D wire $[V(B_3N_3H_6)]_\infty$ exhibited strong half-metallic character relative to its benzene analogue [176]. Both systems are also ferromagnetically

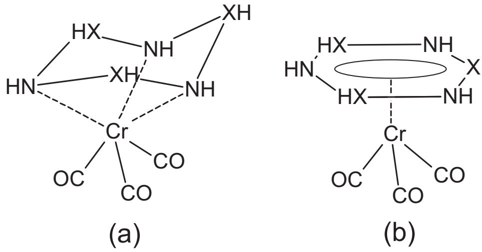

(a) (b)

Fig. 31. Possible (a) η^3 triamine and (b) η^6 delocalized bonding modes for the rings in the complexes $(B_3N_3H_6)Cr(CO)_3$ (X = N, P).

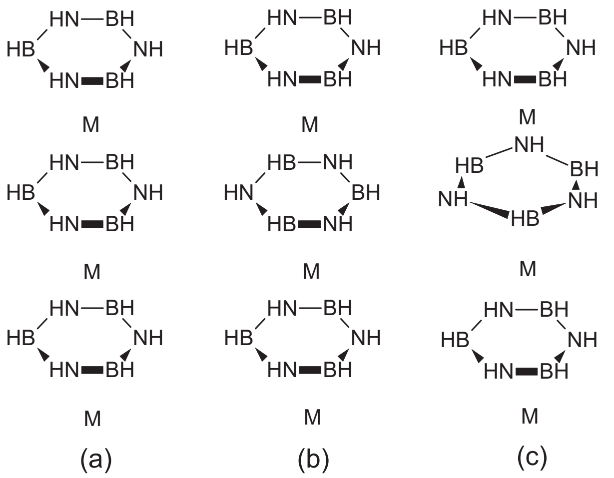

Fig. 32. Structures of three conformations of 1-D $[M(B_3N_3H_6)]_\infty$ (M = transition metal) wires in which (a) the rings are eclipsed with B atoms in all of the rings facing each other, (b) the rings are eclipsed with B atoms in one ring alternately facing N atoms in other rings and (c) the rings are staggered [177].

stable. Another study considers the structural, electronic and magnetic properties of the infinite sandwich molecular wires formed by borazine and the early first-row transition elements Sc, Ti, V, Cr and Mn [177]. It concluded that the $M(B_3N_3H_6)_2$ clusters are energetically stable, especially for M = Sc, Ti and V, and that the infinite molecular wires constructed from them have electronic and magnetic properties similar to their benzene analogues. More specifically, the ground-state electronic structures of the metal-borazine molecular wires formed from both V and Mn are strong half-metallic ferromagnets, those formed by Sc and Cr are non-magnetic metals (semiconductors) and that formed by Ti is an antiferromagnetic metal. In considering the lowest energy of three possible configurations (Fig. 32), it was concluded that the structure in which the B atoms in one ring face the N atoms in the other adjacent rings (Fig. 32b) was most stable for all of the metals except for Mn, for which the structure in which the B atoms in a ring face the B atoms in the other rings (Fig. 32a) was energetically favored.

5.3. *Group 15 element rings*

Calculations show the stability of $(\eta^6\text{-}N_6)M$ (M = Ti, Zr, Hf, Th) due to an interaction of the aromatic 6 π-electron $\eta^6\text{-}N_6$ ring and the metal d and f orbitals, with the aromatic 10 π-electron *cyclo*-$N_6{}^{4-}$ anion present at the ionic limit [54].

In a theoretical study it has been proposed that the half-sandwich complex $(\eta^6\text{-}P_6)V$ with C_{6v} symmetry, and the sandwich complex $(\eta^6\text{-}P_6)_2V$ with D_{6h} symmetry and eclipsed $\eta^6\text{-}P_6$ rings are both stable [178]. The presence of a planar, aromatic *cyclo*-P_6 ligand has been proposed to be present in a theoretical study of $(\eta^6\text{-}C_6H_6)Cr(\eta^6\text{-}P_6)$ [179], while a bridging $\mu\text{-}(\eta^6{:}\eta^6\text{-}P_6)$ ligand (Fig. 33a) is found in X-ray crystal studies of inverse sandwich complexes of Ti [180], V [181], W [181], Nb [124,182] and Mo [183]. Using theoretical data, a structure with bridging $\mu\text{-}(\eta^6{:}\eta^6\text{-}P_6)$ rings that prefer the eclipsed conformation has been proposed for the multi-decker clusters $(\eta^6\text{-}P_6)_{n+1}V_n$ (n = 2–4) [178].

The shape of bridging P_6 ligands depends on the number of complex valence electrons. An undistorted planar ring with approximately D_{6h} symmetry is found in W [181] and Mo [183] complexes with 28 valence electrons. A ring with an in-plane distortion consisting of two short and four long P–P bonds is found in a 26 valence electron V complex [181], while the opposite situation with four short and two long P–P bonds that was characterized as a bis-allylic ring-distortion is found in a 26 valence electron Nb complex [124,182]. Lastly, a puckered ring is present in the 24 valence electron complex $(\eta^5\text{-}C_5Me_5Ti)_2[\mu\text{-}(\eta^3{:}\eta^3\text{-}P_6)]$ (Fig. 33b) [180]. The distances and angles found for the puckered *cyclo*-P_6 unit with the chair-configuration in $(\eta^5\text{-}C_5Me_5Ti)_2[\mu\text{-}(\eta^3{:}\eta^3\text{-}P_6)]$ are similar to those expected for a *cyclo*-$P_6{}^{6-}$ unit [180]. An X-ray crystal study of Th_2P_{11} shows similar nonaromatic and formally *cyclo*-$P_6{}^{-}$ units with the chair-conformation [184] situated between puckered poly-anionic layers of phosphorus atoms. Each *cyclo*-$P_6{}^{-}$ unit acts as a doubly tridentate ligand by forming a triple-decker complex with two Th^{4+} cations that are each located on opposite sides of the ring and bonded to different P atoms. Each Th^{4+} cation has a coordination number of nine produced through interactions with not only the three P atoms of an isolated *cyclo*-$P_6{}^{-}$ unit but also with additional P atoms found in the poly-anionic layers. In contrast, a bicyclic, hexaphosphabenzvalene P_6 unit is bridged by two Th^{4+} cations (Fig. 33c) in the triple-decker complex $(Cp''Th)_2[\mu\text{-}(\eta^3{:}\eta^3\text{-}P_6)]$ ($Cp'' = \eta^5\text{-}(1,3\text{-}{}^tBu_2C_5H_3)$) [185]. A similar structure has been found in the related bicyclic As_6 complex $(Cp''_2Th)_2[\mu\text{-}(\eta^3{:}\eta^3\text{-}As_6)]$ ($Cp'' = \eta^5\text{-}(1,3\text{-}{}^tBu_2C_5H_3)$) [186].

Similar shapes to those found for the bridging P_6 ligand have been proposed for complexes with bridging As_6 ligands [182]. And, indeed, an undistorted $\mu\text{-}(\eta^6{:}\eta^6\text{-}As_6)$ ligand is found in the 28 valence electron complex $[(\eta^5\text{-}C_5Me_4Et)Mo]_2[\mu\text{-}(\eta^6{:}\eta^6\text{-}As_6)]$ [187]. However, in a study of $[(\eta^5\text{-}C_5Me_4R)Co]_2(As_6)$ (R = Me, Et), X-ray crystal data for the R = Me complex shows a nonplanar, butterfly-shaped *cyclo*-As_6 ligand with the Co atom of one $(\eta^5\text{-}C_5Me_5)Co$ unit bonded to four of the As atoms on the outside of one of the wings, and that of the other unit bonded to the four As atoms in the open ends of the wings (Fig. 34) [188].

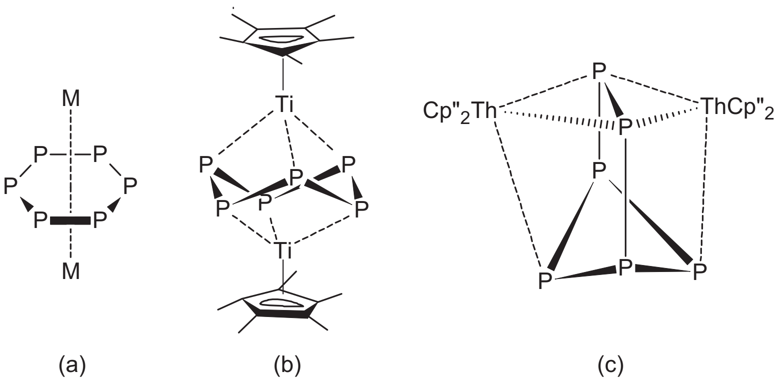

Fig. 33. Structures found for the bridging P_6 ligand in different metal complexes.

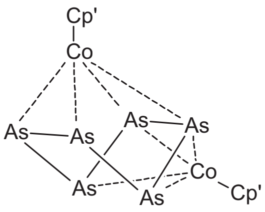

Fig. 34. Single crystal X-ray structure of $[Cp'Co]_2(As_6)$ ($Cp' = \eta^5$-C_5Me_5) [188].

6. *Cyclo*-X_7 ligands

6.1. Group 11 element rings

Calculations show D_{7h} global minimum structures for *cyclo*-X_7^{3-} (X = Cu [189], Ag, Au) [190]. The NICS(1)$_{zz}$ and NICS(2)$_{zz}$ data reported in these studies show that the clusters possess σ-aromatic character due to the presence of 10 valence s-electrons. The addition of a Sc or Y atom to the middle of the planar *cyclo*-Cu_7^{3-} cluster in Cu_7M (M = Sc [189], Y) [190] produces compounds that have enhanced aromaticity and that maintain a global minimum structure D_{7h} symmetry (Fig. 35).

Although Sc, Ti^+ and Zr^+ are too small to be inserted into a *cyclo*-Ag_7^{3-} cluster, a Y atom can be incorporated to produce the Ag_7Y species with a D_{7h} symmetry global minimum structure, and again greater aromaticity than found for the *cyclo*-Ag_7^{3-} cluster [190]. The aromatic Au_7Y cluster has a C_s global minimum structure, but the D_{7h} symmetry structure has an energy that is only 0.02 eV higher than the C_s structure [190].

6.2. Group 13 element rings

Calculations show that while the singlet structure with D_{7h} symmetry is a possible minimum structure for the $[CoB_7]^{2+}$ dication, the other d-block atoms are too large to be encapsulated by the B_7 ring [191].

The B_8^{2-} dianion, in which a planar *cyclo*-B_7 heptagon is centered by a heptacoordinate B atom in the middle of the ring, has a planar D_{7h} symmetry ($^1A_1'$) ground state and exhibits double σ- and π-aromaticity [192,193]. Photoelectron spectroscopic data and theoretical calculations have been interpreted as showing that the structure of the B_8^{2-} dianion in $[LiB_8]^-$ is nearly identical to that of the bare B_8^{2-} dianion except for a slight out-of-plane distortion due to asymmetric capping by the Li^+ cation to produce for $[LiB_8]^-$ a global minimum structure that has C_{7v} symmetry [194]. The stability of the B_8^{2-} unit in $[LiB_8]^-$ was said to indicate that it can serve as a ligand in forming other complexes [194]. Calculations show the stability of the D_{7h} symmetry complexes $(\eta^7$-$BB_7)_2M$ (M = Fe, Co, Ni) in which each 6 π-electron *cyclo*-B_7 heptagon unit is capped by a B atom [151]. It has been suggested [155] that the B_8^{2-} dianion might be stabilized in metal complexes that also contain the η^5-$C_5H_5^-$ ligand.

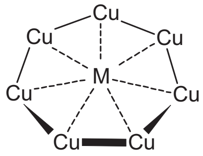

Fig. 35. The stable minimum structure with D_{7h} symmetry calculated for MCu_7 (M = Sc, Y) [190].

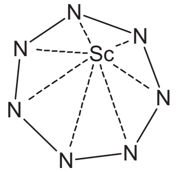

Fig. 36. Local minimum structure with C_{7v} symmetry calculated for $(\eta^7$-$N_7)Sc$ [195].

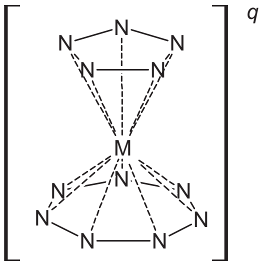

Fig. 37. Local minimum structures calculated for $[N_5MN_7]^q$ (q = 0, M = Ti, Zr, Hf, Th; q = 1-, M = Sc) [196].

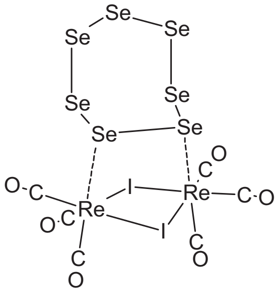

Fig. 38. X-ray crystal structure for $Re_2(\mu$-$I)_2(CO)_6(Se_7)$ [197].

6.3. Group 15 element rings

DFT calculations show the likely existence of $(\eta^7$-$N_7)Sc$ (Fig. 36) with the *cyclo*-N_7 group bonded to Sc through σ, π, and δ interactions [195].

Preliminary but less complete studies indicate that $(\eta^7$-$N_7)La$, $[(\eta^7$-$N_7)Th]^+$ and $(\eta^7$-$N_7)_2Sc$ are stable, while $(\eta^7$-$N_7)Y$, $(\eta^7$-$N_7)Ac$ and $(\eta^7$-$N_7)_2U$ are not [195]. Calculations suggest the stability of the mixed ring compounds $[(\eta^5$-$N_5)M(\eta^7$-$N_7)]^q$ (q = 0, M = Ti, Zr, Hf, Th; q = 1-, M = Sc) (Fig. 37) with the Th complex the most stable [196]. The study also shows that that $[(\eta^5$-$N_5)V(\eta^7$-$N_7)]^+$ is unstable and likely to dissociate into two N_2 molecules, a V atom and one each of N_3 and N_5 [196].

6.4. Group 16 element rings

A bridging *cyclo*-Se_7 group with the chair conformation is 1,2-coordinated to the two Re atoms in $Re_2(\mu$-$I)_2(CO)_6(Se_7)$ (Fig. 38) [197].

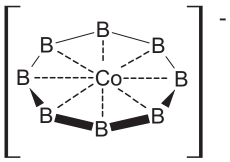

Fig. 39. The global minimum structure of D_{8h} symmetry calculated for $[CoB_8]^-$ [191,198].

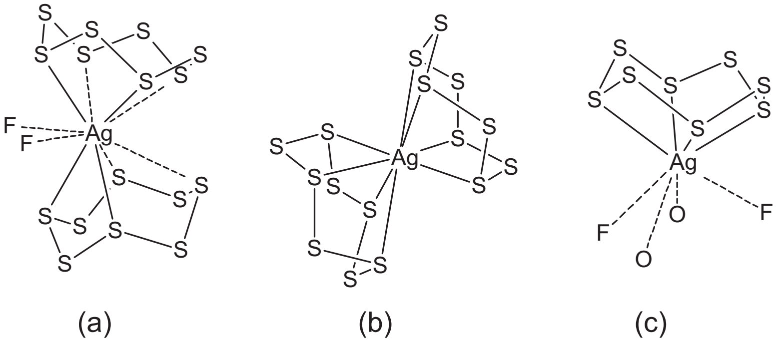

Fig. 40. Solid state X-ray structures of (a) the $[(S_8)_2Ag]^+$ cation in $[(S_8)_2Ag][SbF_6]$ that includes the two F atom contacts with the $[SbF_6]^-$ anion, (b) the $[(S_8)_2Ag]^+$ cation in $[Ag(S_8)_2][Sb(OTeF_5)_6]$ and (c) the $[AgS_8]^+$ cation in $[AgS_8][Al(hfip)_4]$ (hfip = $OCH(CF_3)_2$) including the F and O atom contacts [201].

7. *Cyclo*-X_8 ligands

7.1. Group 13 element rings

A theoretical study of many neutral and charged MB_8 clusters of the first-row transition elements shows that only the smaller atoms (Mn, Fe and Co) can be accommodated within the ring [191], with the singlet state global minimum structure of D_{8h} symmetry found only for $[FeB_8]^{2-}$ and $[CoB_8]^-$ (Fig. 39) [191,198]. Both compounds are doubly aromatic with 6 π and 10 σ radial electrons [191,198].

As with the previously discussed $B_8{}^{2-}$ dianion, it has been suggested [155] that the $B_9{}^-$ anion, in which a planar *cyclo*-B_8 octagon unit is centered by an octacoordinate B atom located in the middle of the B_8 ring [192], might be stabilized in metal complexes that also contain the η^5-$C_5H_5{}^-$ ligand.

7.2. Groups 15 element rings

Preliminary DFT data suggest some bending of the *cyclo*-N_8 units in $(\eta^8\text{-}N_8)_2Th$ [195]. The *cyclo*-$X_8{}^{2-}$ units are centered by the metal ions with crown-like or puckered rather than planar structures in $[X_8M]^q$ (M = Cr, X = As, q = 3- [199]; M = Mo, X = As, q = 2- [199]; M = Mo, X = Sb, q = 3- [199]; M = Nb, X = As, Sb, q = 3- [143]).

7.3. Group 16 element rings

Single crystal X-ray studies show the presence of loosely 1,3-coordinated η^2-S_8 rings and two loosely coordinated monodentate X^- anions in $[(S_8)_2Ag]X$ (X = AsF_6 [200], SbF_6 (Fig. 40a) [201]). Although, to the first order of approximation, X-ray crystal data show the presence of η^4-S_8 rings in $[Ag(S_8)_2][Al(pftb)_4]$ (pftb = $OC(CF_3)_3$) and $[Ag(S_8)_2][Sb(OTeF_5)_6]$ (Fig. 40b), closer examination of the crystal data for $[Ag(S_8)_2][Al(pftb)_4]$ measured at 150 K and 200 K show the presence of two different geometries for each of the two η^4-S_8 rings. The compound $[AgS_8][Al(hfip)_4]$ (hfip = $OCH(CF_3)_2$) also has a structure (Fig. 40c) with an almost η^4-S_8 ring and a $[AgS_8]^+$ group with approximately C_{4v} symmetry [201].

The structure found for the *cyclo*-S_8 unit in $[(S_8)_2Ag]AsF_6$ [200] has also been suggested as a possibility for $[(S_8)_2Cu]^+$ [202]. However, recent calculations have shown that the complexes $[S_8M]^+$ prefer the connectivity $[(S_4)_2M]^+$ (M = Ca, V [202], Cu) [203]. In addition, for M = V, the isomers $[V(S_2)(S_6)]^+$ and $[V[(S_3)(S_5)]^+$ appear to be even more stable [203], similar to what was previously noted for $[(\eta^4\text{-}N_4)_2M]^q$ ((M, q) = (Ni, 0), (Co, 1-), (Fe, 2-)) [52].

A 1,2-coordinated *cyclo*-S_8 unit that bridges two Re atoms is found in $Re_2(\mu\text{-}X)_2(CO)_6(S_8)$ (X = Br, I) [197], while nonplanar 1,3-coordinated and 1,3,5-coordinated S_8 rings are found in two different Rh complexes [204].

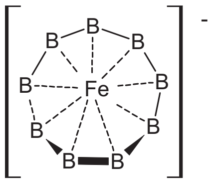

Fig. 41. Global minimum structure of D_{9h} symmetry calculated for $[FeB_9]^-$ [191,198].

8. *Cyclo*-X_9 ligands of Group 13 element rings

A theoretical study shows that the B_9 rings in many neutral and charged MB_9 clusters are versatile in their ability to accommodate first-row transition elements, with the early d-block elements Ti and V slightly too small, and the middle d-block elements Cr and Mn the best geometric matches for the rings [191]. A stable global minimum structure with D_{9h} symmetry has been calculated for $[FeB_9]^-$ (Fig. 41) [191,198]. This compound shows double aromaticity with 6 π and 10 σ radial electrons and its stability is due the presence of both π- and σ-electrons [17]. Analogous structures are not found for CoB_9 and $[NiB_9]^+$. Rather, a nonplanar triplet state structure of C_1 symmetry is preferred by CoB_9 and a nonplanar singlet structure of C_s symmetry is preferred by $[NiB_9]^+$ [198].

9. *Cyclo*-X_{10} ligands of Group 13 element rings

A theoretical study of many neutral and charged MB_{10} clusters of the first-row transition elements shows that the B_{10} rings are only able to interact with larger radii metal atoms such as Sc and Ti. Although the M–B interactions tend to be weak relative to those found in analogous B_n (n = 7–9) ring complexes, the larger number of M–B interactions tend to compensate for this weakness [191].

10. Conclusions

During the last decades of the previous century interest began to develop in cyclic inorganic species of the main group elements that exhibit σ- and π-aromaticity, as well as in metallocene compounds formed from these rings. More recently, with the beginning of the present century, this interest has not only continued to grow but has been extended to the study of analogous species containing rings formed from atoms of the d- and f-block elements. This has led to the discovery of new structures and types of bonding that include δ- and φ-aromaticity [23]. These developments have been pursued using theoretical calculations, experimental procedures or a combination of both approaches.

Inorganic rings, especially of the d- and f-block elements, exhibit some unique differences from their organic counterparts due to an ability to form new types of aromaticity. It is also evident that the study of inorganic rings, as well as their metallocene complexes, can have a unifying influence. Progress is often made by breaking artificial barriers that have been created within and between disciplines, areas of knowledge, or methods of approach. It has therefore been noted that the study of these compounds can provide insights that are necessary for the development of a complete theory of chemical bonding that in turn is applicable to all of chemical science [22].

A goal at the theoretical level has been to find the relative stability of the isomers of particular molecules, with special interest in establishing the global minimum structures. Other goals have been to study the extent to which these compounds exhibit aromatic, antiaromatic and conflicting aromatic behavior, as well as to determine the nature and extent of orbital participation in these types of bonding. This has in turn led to assessments of the accuracy of the different quantitative methods that have been developed to assess aromatic behavior and highlighted the need to both refine and develop even more complete and accurate methods. As this work continues, there may be a need to reevaluate some past computational studies to assess their accuracy.

The aromaticity and stability of inorganic rings can be changed in a variety of ways. As previously shown for organometallic compounds, metal atoms are able to stabilize otherwise unstable organic molecules. Unstable inorganic rings can likewise achieve stability through ionic and covalent interactions with metals.

Several examples have been cited in which the aromaticity of a cyclic inorganic molecules [39,80,90,104,114] or metallocene complexes formed by these rings [43,94,109,123] can be both stabilized and changed through an interaction with alkali metals or, in some examples with alkaline earth metals [77,129]. The reactivity of these compounds can also be altered through this type of interaction [39].

Other examples show that complex stability [92,110,116,117,190,191], ring hapticity [134,136–139] or ring conformation in bis-ring complexes [43,110,111,116,176,177] is influenced by the nature of the transition metal used to form a metallocene complex with a given inorganic ring.

Theoretical studies show that another potential synthetic tool that can change the stability of the inorganic rings or the metallocenes formed from them involves varying the substituents that are placed on the rings [43]. Different ring substituents can also produce changes in the ring conformation in bis-ring complexes [4,105,106].

Several of the cited theoretical and experimental studies show that greater stability can be introduced into inorganic metallocene complexes when cyclopentadienyl rings, alkyl substituted cyclopentadienyl rings or carbonyl ligands are also part of the coordination sphere of a particular transition metal. One study has shown that the stability of some complexes can be achieved by replacing the CO ligand with the even better π acceptor NO^+ ligand [63].

The ability to translate theoretical predictions into synthetic success is only at the initial stages of development. Additional work is needed to prepare predicted theoretical compounds and to test suggested synthetic approaches for these compounds. More study is also needed to determine the reaction mechanisms involved in the formation of desired reaction products [38].

Although the predictions offered in the theoretical studies and the successful synthesis of new complexes are both of value in extending our knowledge and understanding of structure and bonding, the resulting complexes also have several potential practical applications. It is hoped that the continued theoretical and experimental study of these compounds will stimulate further interest in applying this knowledge to the discovery and development of such applications.

As an example, there has already been a great deal of interest in the electronic and magnetic properties of organometallic metallocene compounds that are able to form infinite 1-D, 2-D and 3-D molecular nanowires, crystals and other nanoscale materials that have potential electronic applications [205–207]. Although this work cites some similar studies using inorganic metallocenes [43,95,110,176–178], further work is required to explore their potential use in similar applications. Similarities have also been noted between some of the molecular clusters discussed and potentially useful solid-state materials [208]. Organometallic metallocenes now play an important role as catalysts. Yet to be explored is the ability of inorganic metallocenes to serve a similar role. Equally lacking are studies exploring the use of inorganic metallocenes as reagents in synthetic reactions to create new molecular products or known materials more quickly, more efficiently or in greater yields [40].

Lastly, an understanding of the aromaticity and antiaromaticity of transition metal rings and their metallocene complexes might have relevance in biochemistry for the study of the active cites of enzymes and other biomolecules that contain transition metal atoms and clusters [21].

This active and exciting field of research, due in part to its ability to bridge boundaries found between organic and inorganic chemistry, computational and experimental research, and the theoretical and practical, indeed does seem to provide several avenues by which it can contribute to the continued development of science and technology.

References

[1] (a) Special editions on aromaticity; P.v.R. Schleyer, Guest Ed., Chem. Rev. 101 (5) (2001).;
(b) Chem. Rev. 105 (10) (2005).
[2] M. Faraday, Philos. Trans. R. Soc. Lond. 115 (1825) 440.
[3] A. Kekulé, Bull. Soc. Chim. Fr. 3 (1865) 98.
[4] E. Hückel, Z. Phys. 70 (1931) 204.
[5] W.v.E. Doering, F.L. Detert, J. Am. Chem. Soc. 73 (1951) 876.
[6] R. Breslow, Chem. Eng. News 43 (1965) 90.
[7] R. Breslow, Acc. Chem. Res. 6 (1973) 393.
[8] A. Stanger, Chem. Commun. (2009) 1939.
[9] C.A. Tsipis, Coord. Chem. Rev. 249 (2005) 2740.
[10] C.A. Tsipis, in: G. Parkin (Ed.), Metal–Metal Bonding, Structure and Bonding Book Series, vol. 136, Springer, Berlin/Heidelberg, 2010, p. 217.
[11] A.I. Boldyrev, L.-S. Wang, Chem. Rev. 105 (2005) 3716.
[12] P.v.R. Schleyer, Chem. Rev. 101 (2001) 1115.
[13] P.v.R. Schleyer, H. Jiao, Pure Appl. Chem. 68 (1996) 209.
[14] H.W. Jin, Q.S. Li, Phys. Chem. Chem. Phys. 5 (2003) 1110.
[15] Z. Chen, C.S. Wannere, C. Corminboeuf, R. Puchta, P.v.R. Schleyer, Chem. Rev. 105 (2005) 3842.
[16] B.B. Averkiev, D.Y. Zubarev, L.-M. Wang, W. Huang, L.-S. Wang, A.I. Boldyrev, J. Am. Chem. Soc. 130 (2008) 9248.
[17] B.B. Averkiev, L.-M. Wang, W. Huang, L.-S. Wang, A.I. Boldyrev, Phys. Chem. Chem. Phys. 11 (2009) 9840.
[18] A.N. Alexandrova, A.I. Boldyrev, H.-J. Zhai, L.-S. Wang, Coord. Chem. Rev. 250 (2006) 2811.
[19] J. Chandrasekhar, E.D. Jemmis, P.v.R. Schleyer, Tetrahedron Lett. 20 (1979) 3689.
[20] B.B. Averkiev, A.I. Boldyrev, J. Phys. Chem. A 111 (2007) 12864.
[21] D.Yu. Zubarev, B.B. Averkiev, H.-J. Zhai, L.-S. Wang, A.I. Boldyrev, Phys. Chem. Chem. Phys. 10 (2008) 257.
[22] D.Yu. Zubarev, A.I. Boldyrev, in: E.I. Solomon, R.A. Scott, R.B. King (Eds.), Computational Inorganic and Bioinorganic Chemistry, John Wiley & Sons, Ltd., Chichester, UK, 2009, p. 551.
[23] A.P. Sergeeva, B.B. Averkiev, A.I. Boldyrev, in: G. Parkin (Ed.), Metal–Metal Bonding Structure and Bonding Book Series, vol. 136, Springer, Berlin/Heidelberg, 2010, p. 275.
[24] P.v.R. Schleyer, C. Maerker, A. Dransfeld, H. Jiao, N.J.R.v.E. Hommes, J. Am. Chem. Soc. 118 (1996) 6317.
[25] H. Fallah-Bagher-Shaidaei, C.S. Wannere, C. Corminboeuf, R. Puchta, P.v.R. Schleyer, Org. Lett. 8 (2006) 863.
[26] A.C. Tsipis, Phys. Chem. Chem. Phys. 11 (2009) 8244.
[27] A.C. Tsipis, I.G. Depastas, E.E. Karagiannis, C.A. Tsipis, J. Comp. Chem. 31 (2010) 431.
[28] A.C. Tsipis, I.G. Depastas, C.A. Tsipis, Symmetry 2 (2010) 284.
[29] D.Yu. Zubarev, A.I. Boldyev, Phys. Chem. Chem. Phys. 10 (2008) 5207.
[30] A.P. Sergeeva, A.I. Boldyrev, Comments Inorg. Chem. 31 (2010) 2.

[31] P.F. Weck, A.P. Sergeeva, E. Kim, A.I. Boldyrev, K.R. Czerwinski, Inorg. Chem. 50 (2011) 1039.

[32] T.J. Kealy, P.L. Pauson, Nature 168 (1951) 1039.

[33] S.A. Miller, J.A. Tebboth, J.F. Tremaine, J. Chem. Soc. (1952) 632.

[34] A. Stock, E. Pohland, Chem. Ber. 59B (1926) 2215.

[35] D.R. Roy, P.K. Chattaraj, J. Phys. Chem. A 112 (2008) 1612.

[36] P.K. Chattaraj, D.R. Roy, S. Duley, Chem. Phys. Lett. 460 (2008) 382.

[37] A.E. Kuznetsov, A.I. Boldyrev, Chem. Phys. Lett. 388 (2004) 452.

[38] J.O.C. Jiménez-Halla, E. Matito, J. Robles, M. Solà, J. Organometal. Chem. 691 (2006) 4359.

[39] J.O.C. Jiménez-Halla, E. Matito, L. Blancafort, J. Robles, M. Solà, J. Comp. Chem. 30 (2009) 2764.

[40] P.K. Chattaraj, S. Giri, J. Mol. Struct. (THEOCHEM) 865 (2008) 53.

[41] E.D. Jemmis, G. Subramanian, G.N. Srinivas, Inorg. Chem. 33 (1994) 2317.

[42] R.J. Wright, M. Brynda, P.R. Power, Angew. Chem. Int. Ed. 45 (2006) 5953.

[43] J.M. Mercero, M. Piris, J.M. Matxain, X. Lopez, J.M. Ugalde, J. Am. Chem. Soc. 131 (2009) 6949.

[44] D.-K. Seo, J.D. Corbett, Science 291 (2001) 841.

[45] A. Purath, R. Köppe, H. Schnöckel, Angew. Chem. Int. Ed. 38 (1999) 2926.

[46] P. Yang, R. Köppe, T. Duan, J. Hartig, G. Hadiprono, B. Pilawa, I. Keilhauer, H. Schnöckel, Angew. Chem. Int. Ed. 46 (2007) 3579.

[47] G.N. Srinivas, A. Anoop, E.D. Jemmis, T.P. Hamilton, K. Lammertsma, J. Leszczynski, H.F. Schaefer III, J. Am. Chem. Soc. 112 (2003) 16397.

[48] D. Mallick, P. Parameswaran, E.D. Jemmis, J. Phys. Chem. A 112 (2008) 13080.

[49] X.-W. Li, W.T. Pennington, G.H. Robinson, J. Am. Chem. Soc. 117 (1995) 7578.

[50] X.-W. Li, Y. Xie, P.R. Schreiner, K.D. Gripper, R.C. Crittendon, C.F. Campana, H.F. Schaefer, G.H. Robinson, Organometallics 15 (1996) 3798.

[51] G.N. Srinivas, L. Yu, M. Schwartz, Organometallics 20 (2001) 5200.

[52] L. Jin, Yi-H. Ding, J. Phys. Chem. A 113 (2009) 5246.

[53] N.C. Baird, J. Am. Chem. Soc. 94 (1972) 4941.

[54] M. Straka, Chem. Phys. Lett. 358 (2002) 531.

[55] M. Di Vaira, P. Stoppioni, M. Peruzzini, Polyhedron 6 (1987) 351.

[56] S. Umbarkar, P. Sekar, M. Scheer, J. Chem. Soc. Dalton Trans. (2000) 1135.

[57] B.M. Cossairt, C.C. Cummins, J. Am. Chem. Soc. 131 (2009) 15501.

[58] H.A. Spinney, N.A. Piro, C.C. Cummins, J. Am. Chem. Soc. 131 (2009) 16233.

[59] O.J. Scherer, Angew. Chem. Int. Ed. Engl. 29 (1990) 1104.

[60] A.-J. DiMaio, A.L. Rheingold, Chem. Rev. 90 (1990) 169.

[61] C.A. Ghilardi, S. Midollini, A. Orlandini, L. Sacconi, Inorg. Chem. 19 (1980) 301.

[62] H.J. Breunig, R. Rösler, E. Lork, Angew. Chem. Int. Ed. Engl. 36 (1997) 2819.

[63] B. Flemmig, P.T. Wolczanski, R. Hoffmann, J. Am. Chem. Soc. 127 (2005) 1278.

[64] B.M. Cossairt, M.-C. Diawara, C.C. Cummins, Science 323 (2009) 602.

[65] C. Bianchini, M. Di Vaira, A. Meli, L. Sacconi, J. Am. Chem. Soc. 103 (1981) 1448.

[66] M. Di Vaira, S. Midollini, L. Sacconi, J. Am. Chem. Soc. 101 (1979) 1757.

[67] J.W. Lauher, M. Elian, R.H. Summerville, R. Hoffmann, J. Am. Chem. Soc. 98 (1976) 3219.

[68] M. Di Vaira, M.P. Ehses, M. Peruzzini, P. Stoppioni, Polyhedron 18 (1999) 2331.

[69] F. Cecconi, C.A. Ghilardi, S. Midollini, A. Orlandini, Angew. Chem. Suppl. (1983) 718.

[70] M. Di Vaira, P. Stoppioni, M. Peruzzini, J. Chem. Soc. Dalton Trans. (1990) 109.

[71] D. Fenske, J. Hachgenei, Angew. Chem. Int. Ed. Engl. 25 (1986) 175.

[72] R. Faggiani, R.J. Gillespie, C. Campana, J.W. Kolis, J. Chem. Soc., Chem. Commun. (1987) 485.

[73] A. Seigneurin, T. Makani, D.J. Jones, J. Rozière, J. Chem. Soc. Dalton Trans. (1987) 2111.

[74] A.C. Tsipis, C.A. Tsipis, J. Am. Chem. Soc. 127 (2005) 10623.

[75] H.-J. Zhai, B.B. Averkiev, D.Yu. Zubarev, L.-S. Wang, A.I. Boldyrev, Angew. Chem. Int. Ed. 46 (2007) 4277.

[76] A.C. Tsipis, C.E. Kefalidis, C.A. Tsipis, J. Am. Chem. Soc. 130 (2008) 9144.

[77] S.-D. Li, C.-Q. Miao, J.-C. Guo, Eur. J. Inorg. Chem. (2008) 1205.

[78] N.N. Greenwood, C.G. Savory, R.N. Grimes, L.D. Sneddon, A. Davison, S.S. Wreford, J. Chem. Soc., Chem. Commun. (1974) 718.

[79] V.R. Miller, R.N. Grimes, J. Am. Chem. Soc. 95 (1973) 5078.

[80] X. Li, A.E. Kuznetsov, H.-F. Zhang, A.I. Boldyrev, L.-S. Wang, Science 291 (2001) 859.

[81] J.C. Santos, W. Tiznado, R. Contreras, P. Fuentealba, J. Chem. Phys. 120 (2004) 1670.

[82] J. Jusélius, M. Straka, D. Sundholm, J. Phys. Chem. A 105 (2001) 9939.

[83] R.W.A. Havenith, P.W. Fowler, E. Steiner, S. Shetty, D. Kanhere, S. Pal, Phys. Chem. Chem. Phys. 6 (2004) 285.

[84] Y.-C. Lin, J. Jusélius, D. Sundholm, J. Gauss, J. Chem. Phys. 122 (2005) 214308.

[85] C. Mang, C. Liu, J. Zhou, Z. Li, K. Wu, Chem. Phys. Lett. 438 (2007) 20.

[86] M. Mandado, A. Krishtal, C.V. Alsenoy, P. Bultinck, J.M. Hermida-Ramón, J. Phys. Chem. A 111 (2007) 11885.

[87] P.W. Fowler, R.W.A. Havenith, E. Steiner, Chem. Phys. Lett. 342 (2001) 85.

[88] A.E. Kuznetsov, A.I. Boldyrev, X. Li, L.-S. Wang, J. Am. Chem. Soc. 123 (2001) 8825.

[89] A.I. Boldyrev, A.E. Kuznetsov, Inorg. Chem. 41 (2002) 532.

[90] A.E. Kuznetsov, K.A. Birch, A.I. Boldyrev, X. Li, H.-J. Zhari, L.-S. Wang, Science 300 (2003) 622.

[91] Z. Chen, C. Corminboeuf, T. Heine, J. Bohmann, P.v.R. Schleyer, J. Am. Chem. Soc. 125 (2003) 13930.

[92] J.M. Mercero, E. Formoso, J.M. Matxain, L.A. Eriksson, J.M. Ugalde, Chem. Eur. J. (2006) 4495.

[93] L.-M. Yang, C.-B. Shao, Y.-H. Ding, C.-C. Sun, Phys. Chem. Chem. Phys. 10 (2008) 2020.

[94] A. Datta, S.S. Mallajosyula, S.K. Pati, Acc. Chem. Res. 40 (2007) 213.

[95] L.-M. Yang, J. Wang, Y.-H. Ding, C.-C. Sun, Organometallics 26 (2007) 4449.

[96] M.-D. Su, S.-Y. Chu, J. Phys. Chem. 95 (1991) 9757.

[97] A.J. Bridgeman, J. Rothery, Inorg. Chim. Acta 288 (1999) 17.

[98] B. Kaufmann, H. Nöth, R.T. Paine, K. Polborn, M. Thomann, Angew. Chem. Int. Ed. Engl. 32 (1993) 1446.

[99] G. Linti, H. Nöth, R.T. Paine, Chem. Ber. 126 (1993) 875.

[100] C.E. Jones Jr., P.A. Clayborne, J.U. Reveles, J.J. Melko, U. Gupta, S.N. Khanna, A.W. Castleman Jr., J. Phys. Chem. A 112 (2008) 13316.

[101] J.J. Melko, P.A. Clayborne, C.E. Jones Jr., J.U. Reveles, U. Gupta, S.N. Khanna, A.W. Castleman Jr., J. Phys. Chem. A 114 (2010) 2045.

[102] M. Benard, Nouv. J. Chim. 10 (1986) 529.

[103] W.G. Xu, Y.C. Zhang, S.X. Lu, R.C. Zhang, J. Mol. Struct. (THEOCHEM) 900 (2009) 44.

[104] H.-J. Zhai, A.E. Kuznetsov, A.I. Boldyrev, L.-S. Wang, ChemPhysChem 5 (2004) 1885.

[105] K. Takanashi, V.Y. Lee, M. Ichinohe, A. Sekiguchi, Angew. Chem. Int. Ed. 45 (2006) 3269.

[106] K. Takanashi, V.Y. Lee, A. Sekiguchi, Organometallics 28 (2009) 1248.

[107] K. Takanashi, V.Y. Lee, M. Ichinohe, A. Sekiguchi, Eur. J. Inorg. Chem. (2007) 5471.

[108] K. Takanashi, V.Y. Lee, T. Matsuno, M. Ichinohe, A. Sekiguchi, J. Am. Chem. Soc. 127 (2005) 5768.

[109] V.Y. Lee, K. Takanashi, A. Sekiguchi, Dalton Trans. 39 (2010) 9229.

[110] J.M. Mercero, J.M. Matxain, J.M. Ugalde, Angew. Chem. Int. Ed. 43 (2004) 5485.

[111] Q.S. Li, J. Guan, J. Phys. Chem. A 107 (2003) 8584.

[112] J. Guan, Q. Li, J. Phys. Chem. A 109 (2005) 9875.

[113] L. Jin, Yi-H. Ding, J. Phys. Chem. A 113 (2009) 13645.

[114] A.E. Kuznetsov, H.-J. Zhai, L.-S. Wang, A.I. Boldyrev, Inorg. Chem. 41 (2002) 6062.

[115] M. Yi, K. Fisher, I. Dance, New J. Chem. 25 (2001) 73.

[116] Z. Li, C. Zhao, L. Chen, J. Mol. Struct. (THEOCHEM) 810 (2007) 1.

[117] O.J. Scherer, J. Vondung, G. Wolmershäuser, Angew. Chem. Int. Ed. Engl. 28 (1989) 1355.

[118] O.J. Scherer, R. Winter, G. Wolmershäuser, Z. Anorg, Allg. Chem. 619 (1993) 827.

[119] M. Scheer, E. Herrmann, J. Sieler, M. Oehme, Angew. Chem. Int. Ed. Engl. 30 (1991) 969.

[120] M.E. Barr, S.K. Smith, B. Spencer, L.F. Dahl, Organometallics 10 (1991) 3983.

[121] M. Scheer, M. Dargatz, P.G. Jones, J. Organometal. Chem. 447 (1993) 259.

[122] C.v. Hänisch, D. Fenske, F. Weigend, R. Ahlrichs, Chem. Eur. J. 3 (1997) 1494.

[123] Z. Li, W. Wu, S. Li, J. Mol. Struct. (THEOCHEM) 908 (2009) 73.

[124] M.J. Collins, R.J. Gillespie, J.W. Kolis, J.F. Sawyer, Inorg. Chem. 25 (1986) 2057.

[125] J. Beck, J. Solid State Chem. 125 (1996) 165.

[126] E. Ahmed, E. Ahrens, M. Heise, M. Ruck, Z. Anorg, Allg. Chem. 636 (2010) 2602.

[127] B. Le Guennic, H. Jiao, S. Kahlal, J.-Y. Saillard, J.-F. Halet, S. Ghosh, M. Shang, A.M. Beatty, A.L. Rheingold, T.P. Fehlner, J. Am. Chem. Soc. 126 (2004) 3203.

[128] M.-D. Su, S.-Y. Chu, J. Phys. Chem. 93 (1989) 6043.

[129] A.P. Sergeeva, A.I. Boldyrev, Organometallics 29 (2010) 3951.

[130] T. Kudo, S. Nagase, J. Mol. Struct. (THEOCHEM) 311 (1994) 111.

[131] L. Yong, S.D. Hoffmann, T.F. Fässler, S. Riedel, M. Kaupp, Angew. Chem. Int. Ed. 44 (2005) 2092.

[132] H.-J. Zhai, L.-S. Wang, A.E. Kuznetsov, A.I. Boldyrev, J. Phys. Chem. A 106 (2002) 5600.

[133] M. Lein, J. Frunzke, G. Frenking, Angew. Chem. Int. Ed. 42 (2003) 1303.

[134] G. Frison, F. Mathey, A. Sevin, J. Phys. Chem. A 106 (2002) 5653.

[135] M. Lein, J. Frunzke, A. Timoshkin, G. Frenking, Chem. Eur. J. 7 (2001) 4155.

[136] M. Lein, J. Frunzke, G. Frenking, Inorg. Chem. 42 (2003) 2504.

[137] J. Frunzke, M. Lein, G. Frenking, Organometallics 21 (2002) 3351.

[138] A.C. Tsipis, A.Th. Chaviara, Inorg. Chem. 43 (2004) 1273.

[139] L.A. Burke, R.N. Butler, J.C. Stephens, Chem. Soc., Perkin Trans. 2 (2001) 1679.

[140] E.J.P. Malar, Inorg. Chem. 42 (2003) 3873.

[141] E. Urnėžius, W.W. Brennessel, C.J. Cramer, J.E. Ellis, R.v.R. Schleyer, Science 295 (2002) 832.

[142] Z.-Z. Liu, W.-Q. Tian, J.-K. Feng, G. Zhang, W.-Q. Li, J. Phys. Chem. A 109 (2005) 5645.

[143] B. Kesanli, J. Fettinger, B. Scott, B. Eichhorn, Inorg. Chem. 43 (2004) 3840.

[144] L. Nyulászi, Chem. Rev. 101 (2001) 1229.

[145] H.J. Breunig, N. Burford, R. Rösler, Angew. Chem. Int. Ed. 39 (2000) 4148.

[146] E.J.P. Malar, Theor. Chem. Acc. 114 (2005) 213.

[147] W. Tremel, R. Hoffmann, M. Kertesz, J. Am. Chem. Soc. 111 (1989) 2030.

[148] B. Rink, O.J. Scherer, G. Heckmann, G. Wolmershäuser, Chem. Ber. 125 (1992) 1011.

[149] P. Sekar, M. Scheer, A. Voigt, R. Kirmse, Organometallics 18 (1999) 2833.

[150] P. Sekar, S. Umbarkar, M. Scheer, A. Voigt, R. Kirmse, Eur. J. Inorg. Chem. (2000) 2585.

[151] S.-D. Li, J.-C. Guo, C.-Q. Miao, G.-M. Ren, Angew. Chem. Int. Ed. 44 (2005) 2158.

[152] S.-D. Li, C.-Q. Miao, G.-M. Ren, J.-C. Guo, Eur. J. Inorg. Chem. (2006) 2567.

[153] S.-D. Li, C.-Q. Miao, J.-C. Guo, J. Phys. Chem. A 111 (2007) 12069.

[154] S. Shahbazian, S. Alizadeh, J. Phys. Chem. A 112 (2008) 10365.

[155] L.-M. Yang, H.-P. He, Y.-H. Ding, C.-C. Sun, Organometallics 27 (2008) 1727.

[156] S.K. Bose, S. Ghosh, B.C. Noll, J.-F. Halet, J.-Y. Saillard, A. Vega, Organometallics 26 (2007) 5377.

[157] S. Sahoo, K.H.K. Reddy, R.S. Dhayal, S.M. Mobin, V. Ramkumar, E.D. Jemmis, S. Ghosh, Inorg. Chem. 48 (2009) 6509.

[158] S. Ghosh, A.M. Beatty, T.P. Fehlner, J. Am. Chem. Soc. 123 (2001) 9188.

[159] S. Ghosh, M. Shang, T.P. Fehlner, J. Am. Chem. Soc. 121 (1999) 7451.

[160] P.v.R. Schleyer, H. Jiao, J.R. van Eikema Hommes, V.G. Malkin, O.L. Malkina, J. Am. Chem. Soc. 119 (1997) 12669.
[161] P.W. Fowler, E. Steiner, J. Phys. Chem. A 101 (1997) 1409.
[162] E.D. Jemmis, B. Kiran, Inorg. Chem. 37 (1998) 2110.
[163] B. Chiavarino, M.E. Crestoni, A.D. Marzio, S. Fornarini, M. Rosi, J. Am. Chem. Soc. 121 (1999) 11204.
[164] A. Soncini, C. Domene, J.J. Engelberts, P.W. Fowler, A. Rassat, J.H. van Lenthe, R.W.A. Havenith, L.W. Jenneskens, Chem. Eur. J. 11 (2005) 1257.
[165] H.S. Kang, J. Phys. Chem. A 109 (2005) 1458.
[166] J.J. Engelberts, R.W.A. Havenith, J.H. van Lenthe, L.W. Lenneskens, P.W. Fowler, Inorg. Chem. 44 (2005) 5266.
[167] W. Shen, M. Li, Y. Li, S. Wang, Inorg. Chim. Acta 360 (2007) 619.
[168] B. Kiran, A.K. Phukan, E.D. Jemmis, Inorg. Chem. 40 (2001) 3615.
[169] A.K. Phukan, R.P. Kalagi, S.R. Gadre, E.D. Jemmis, Inorg. Chem. 43 (2004) 5824.
[170] R. Islas, E. Chamorro, J. Robles, T. Heine, J.C. Santos, G. Merino, Struct. Chem. 18 (2007) 833.
[171] I. Fernández, G. Frenking, Faraday Discuss. 135 (2007) 403.
[172] P.W. Fowler, D.E. Bean, M. Seed, J. Phys. Chem. A 114 (2010) 10742.
[173] A.J. Bridgeman, Polyhedron 17 (1998) 2279.
[174] G. Huttner, B. Krieg, Chem. Ber. 105 (1972) 3437.
[175] B. Kaufmann, N. Metzler, H. Nöth, R.T. Paine, Chem. Ber. 127 (1994) 825.
[176] S.S. Mallajosyula, S. Sairam, P. Parida, K.S. Pati, J. Mater. Chem. 19 (2009) 1761.
[177] L. Zhu, J. Wang, J. Phys. Chem. C 113 (2009) 8767.
[178] J. Wang, X. Zhang, P.v.R. Schleyer, Z. Chen, J. Chem. Phys. 128 (2008) 104706.
[179] M.C. Kerins, N.J. Fitzpatrick, M.T. Nguyen, Polyhedron 8 (1989) 1135.
[180] O.J. Scherer, H. Swarowsky, G. Wolmershäuser, W. Kaim, S. Kohlmann, Angew. Chem. Int. Ed. Engl. 26 (1987) 1153.
[181] O.J. Scherer, J. Schwalb, H. Swarowsky, G. Wolmershäuser, W. Kaim, R. Gross, Chem. Ber. 121 (1988) 443.
[182] A.C. Reddy, E.D. Jemmis, O.J. Scherer, R. Winter, G. Heckmann, G. Wolmershäuser, Organometallics 11 (1992) 3894.
[183] O.J. Scherer, H. Sitzmann, G. Wolmershäuser, Angew. Chem. Int. Ed. Engl. 24 (1985) 351.
[184] H.-G.v. Schnering, M. Wittmann, R.J. Nesper, Less Common Met. 76 (1980) 213.
[185] O.J. Scherer, B. Werner, G. Heckmann, G. Wolmershäuser, Angew. Chem. Int. Ed. Engl. 30 (1991) 553.
[186] O.J. Scherer, J. Schulze, G. Wolmershäuser, J. Organometal. Chem. 484 (1994) C5.
[187] O.J. Scherer, H. Sitzmann, G. Wolmershäuser, Angew. Chem. Int. Ed. Engl. 28 (1989) 212.
[188] O.J. Scherer, K. Pfeiffer, G. Heckmann, J. Organometal. Chem. 425 (1992) 141.
[189] T. Höltzl, E. Janssens, N. Veldeman, T. Veszprémi, P. Lievens, M.T. Nguyen, ChemPhysChem 9 (2008) 833.
[190] L. Lin, P. Lievens, M.T. Nguyen, J. Mol. Struct. (THEOCHEM) 943 (2010) 23.
[191] Z. Pu, K. Ito, P.v.R. Schleyer, Q.-S. Li, Inorg. Chem. 48 (2009) 10679.
[192] D.Yu. Zubarev, A.I. Boldyrev, J. Comput. Chem. 28 (2006) 251.
[193] P.W. Fowler, B.R. Gray, Inorg. Chem. 46 (2007) 2892.
[194] A.N. Alexandrova, H.-J. Zhai, L.-S. Wang, A.I. Boldyrev, Inorg. Chem. 43 (2004) 3552.
[195] L. Gagliardi, P. Pyykkö, J. Am. Chem. Soc. 123 (2001) 9700.
[196] L. Gagliardi, P. Pyykkö, J. Phys. Chem. A 106 (2002) 4690.
[197] A. Bacchi, W. Baratta, F. Calderazzo, F. Marchetti, G. Pelizzi, Inorg. Chem. 41 (2002) 3894.
[198] K. Ito, Z. Pu, Q.-S. Li, P.v.R. Schleyer, Inorg. Chem. 47 (2008) 10906.
[199] B. Kesanli, J. Fettinger, B. Eichhorn, J. Am. Chem. Soc. 125 (2003) 7367.
[200] H.W. Roesky, M. Thomas, J. Schimkowiak, P.G. Jones, W. Pinkert, G.M. Sheldrick, J. Chem. Soc., Chem. Commun. (1982) 895.
[201] T.S. Cameron, A. Decken, I. Dionne, M. Fang, I. Krossing, J. Passmore, Chem. Eur. J. 8 (2002) 3386.
[202] I. Dance, K. Fisher, G. Willett, Angew. Chem. Int. Ed. Engl. 34 (1995) 201.
[203] Y. Steudel, M.W. Wong, R. Steudel, Eur. J. Inorg. Chem. (2005) 2514.
[204] F.A. Cotton, E.V. Dikarev, M.A. Petrukhina, Angew. Chem. Int. Ed. 40 (2001) 1521.
[205] L. Wang, X. Gao, X. Yan, J. Zhou, Z. Gao, S. Nagase, S. Sanvito, Y. Maeda, T. Akasaka, W.N. Mei, J. Lu, J. Phys. Chem. C 114 (2010) 21893.
[206] A. Pramanik, H.S. Kang, J. Phys. Chem. A 115 (2011) 219.
[207] X. Zhang, Z. Tian, S.-W. Yang, J. Wang, J. Phys. Chem. C 115 (2011) 2948.
[208] R. Gautier, J.-F. Halet, J.-Y. Saillard, in: E.I. Solomon, R.A. Scott, R.B. King (Eds.), Computational Inorganic and Bioinorganic Chemistry, John Wiley & Sons, Ltd., Chichester, UK, 2009, p. 433.